



HAL
open science

Neuroprotective effects of Myricetin on Epoxiconazole-induced toxicity in F98 cells

Hiba Hamdi, Salwa Abid-Essefi, Joel Eyer

► To cite this version:

Hiba Hamdi, Salwa Abid-Essefi, Joel Eyer. Neuroprotective effects of Myricetin on Epoxiconazole-induced toxicity in F98 cells. *Free Radical Biology and Medicine*, 2021, 164, pp.154-163. 10.1016/j.freeradbiomed.2020.12.451 . hal-03129683

HAL Id: hal-03129683

<https://hal.science/hal-03129683>

Submitted on 3 Feb 2023

HAL is a multi-disciplinary open access archive for the deposit and dissemination of scientific research documents, whether they are published or not. The documents may come from teaching and research institutions in France or abroad, or from public or private research centers.

L'archive ouverte pluridisciplinaire **HAL**, est destinée au dépôt et à la diffusion de documents scientifiques de niveau recherche, publiés ou non, émanant des établissements d'enseignement et de recherche français ou étrangers, des laboratoires publics ou privés.



Distributed under a Creative Commons Attribution - NonCommercial 4.0 International License

1 **Neuroprotective effects of Myricetin on Epoxiconazole-induced toxicity in F98 cells**

2

3

4 Hiba Hamdi^{a, b}, Salwa Abid-Essefi^a, Joel Eyer^{c *}

5

6

7 ^aLaboratory for Research on Biologically Compatible Compounds, Faculty of Dental
8 Medicine, University of Monastir, Avicenne Street, 5019 Monastir, Tunisia.

9 ^bHigher Institute of Biotechnology, University of Monastir, Tunisia.

10 ^cLaboratoire Micro et Nanomédecines Translationnelles (MINT), Inserm 1066, CNRS 6021,
11 Institut de Biologie de la Santé, Centre Hospitalier Universitaire, 49033 Angers, France.

12

13

14

15

16

17

18

19

20

21

22

23

24

25

26 ***Corresponding author: Joel Eyer**

27 Laboratoire Micro et Nanomédecines Translationnelles (MINT), Inserm 1066, CNRS 6021,
28 Institut de Biologie de la Santé, Centre Hospitalier Universitaire, 49033 Angers, France.

29 E-mail: joel.eyer@univ-angers.fr

30 Tel: 33 (0)2.44.68.84.88

31 Fax: 33 (0)2.44.68.84.89

32

33

34 **Abstract**

35 Epoxiconazole is one of the most commonly used fungicides in the world. The exposition of
36 humans to pesticides is mainly attributed to its residue in food or occupational exposure in
37 agricultural production. Because of its lipophilic character, Epoxiconazole can accumulate in
38 the brain [1]. Consequently, it is urgent to explore efficient strategies to prevent or treat
39 Epoxiconazole-related brain damages. The use of natural molecules commonly found in our
40 diet represents a promising avenue. Flavonoids belong to a major sub-group compounds
41 possessing powerful antioxidant activities based on their different structural and sterical
42 properties [2]. We choose to evaluate Myricetin, a flavonoid with a wide spectrum of
43 pharmacological effects, for its possible protective functions against Epoxiconazole-induced
44 toxicities. The cytotoxicity induced by this fungicide was evaluated by the cell viability, cell
45 cycle arrest, ROS generation, antioxidant enzyme activities, and Malondialdehyde production,
46 as previously described in Hamdi et al. 2019 [3]. The apoptosis was assessed through the
47 evaluation of the mitochondrial transmembrane potential ($\Delta\Psi_m$), caspases activation, DNA
48 fragmentation, cytoskeleton disruption, nuclear condensation, appearance of sub-G0/G1 peak
49 (fragmentation of the nucleus) and externalization of Phosphatidylserine. This study indicates
50 that pre-treatment of F98 cells with Myricetin during two hours before Epoxiconazole
51 exposure significantly increased the survival of cells, restored DNA synthesis of the S phase,
52 abrogated the ROS generation, regulated the activities of Catalase (CAT) and Superoxide
53 Dismutase (SOD), and reduced the MDA level. The loss of mitochondrial membrane
54 potential, DNA fragmentation, cytoskeleton disruption, chromatin condensation,
55 Phosphatidylserine externalization, and Caspases activation were also reduced by Myricetin.
56 Together, these findings indicate that Myricetin is a powerful natural product able to protect
57 cells from Epoxiconazole-induced cytotoxicity and apoptosis.

58

59 **Keywords:** Epoxiconazole, Myricetin, Oxidative stress, Apoptosis, DNA fragmentation,
60 Cytoskeleton disruption.

61

62

63 **List of Abbreviations:** EPX: Epoxiconazole; MYR: Myricetin; ROS: Reactive Oxygen
64 Species; $\Delta\Psi_m$: Mitochondrial Transmembrane Potential; IC50: Inhibitory Concentration of
65 50% of the population; PBS: Phosphate Buffer Saline; DCFH-DA: 2, 7-Dichlorofluoresce
66 Diacetate; FCS: Fetal Calf Serum; MTT: 3-(4, 5-Dimethylthiazol-2-yl), 2, 5-
67 Diphenyltetrazolium Bromide; DMSO: Dimethylsulfoxide; PI: Propidium Iodide; Rh-123:
68 Rhodamine 123; H₂O₂: Hydrogen Peroxide; MDA: Malondialdehyde; DO: Optical Density;
69 GSH: Glutathione; CAT: Catalase; SOD: Superoxide dismutase; V:V: Volume:volume, NAC:
70 N acetylcysteine; H₂O₂: hydrogen peroxide.

71

72

73 **Introduction**

74 Although the large spectrum use of pesticides for pest control, these products represent a risk
75 of poisoning for food and agricultural security [4-5]. In particular, Triazole fungicides have
76 appeared as a category of pollutants widely applied in various sectors, including agricultural,
77 industrial, and pharmaceutical sectors [6-7]. Their mode of action is the inhibition of a
78 specific enzyme of the fungus Cytochrome P450 (CYP: lanosterol-14 α -demethylase), which
79 is important for the synthesis of the fungal membrane [8]. Triazole fungicides are
80 characterized by their chemical stability, their low biodegradability and also by their strong
81 bioaccumulation [9-11]. Various effects of Triazole fungicides have been demonstrated in
82 diverse toxicological studies; these chemicals have been shown to be hepatotoxic,
83 tumorigenic, teratogenic, endocrine disruptors, genotoxic, and neurotoxic. In particular,
84 Triazole fungicides exposure affects the mammalian nervous system, inducing
85 neurobehavioral deficits and neuropathology [12]. One neurotoxic effect of these compounds
86 is the alteration of the dopaminergic neurotransmission, via the inhibition of depolarization-
87 evoked Ca²⁺influx [13].

88 Epoxiconazole (EPX) is a widely used synthetic fungicide, which aims to stop the
89 biosynthesis of the steroid ergosterol, an essential component of the fungal membrane, by
90 competitively inhibiting the enzyme lanosterol 14 α -demethylase [14]. It belongs to pesticides
91 having “risky” properties: very high bioaccumulation potential with log KOW > 3, strong
92 adsorption in soil with Koc 68 > 500, and long persistency with DT50 > 30 [15]. Combining
93 its properties with increased levels of usage explains the long-term residues of EPX in soils of
94 Europe [16-18]. In addition, it is highly persistent in soil (half-life in soil of over 1500 days)
95 [19-20]. The analysis of soil 7 days after EPX application showed that the residual
96 concentrations of this pesticide were about 0.11-0.35 mg/kg [21]. Following repeated
97 applications, this pollutant enters freshwater ecosystems. Otherwise, EPX has been detected in
98 aquatic environments and wastewaters [22-24], as well as in agricultural topsoils [25].
99 Previous studies have shown that the potential target of Triazole fungicides is the
100 mitochondrion. Mitochondrial dysfunction would lead to energy depletion, modulation of
101 autophagy, followed by programmed cell death [26]. In line with these findings, we recently
102 showed that EPX is particularly toxic for cells of the nervous system, like F98 cells, where it
103 produces cell cycle arrest, cytoskeleton disruption, and DNA damage. It also alters
104 mitochondrial function and provokes apoptosis via caspases dependent signaling pathway.
105 Finally, EPX induces ROS generation and lipid peroxidation [3]. Such oxidative stress is a

106 major cause of neurotoxicant-associated cellular damage, and ROS production during
107 oxidative stress has been reported to initiate signaling cascades leading to apoptosis in
108 Parkinson's disease [27].

109 We used the F98 cells due to their biological resemblance with primary astrocytes and their
110 broad use as an astrocyte cell model and also because of their large size, which allows clear-
111 cut microscopic evaluation of the effects of EPX on organelles, in particular the cytoskeleton
112 and mitochondria. Moreover, because of their strong and well-characterized proliferative
113 properties, it is a convenient model for precise evaluation of the cell cycle and survival.
114 Flavonoids are ubiquitous in nature and abundant in food, providing an essential source for
115 the prevention of chronic diseases, including cancer [28]. In particular, Myricetin (MYR) is a
116 Flavonoid compound enriched in fruits and vegetables, with antioxidants [29], anti-tumor [30-
117 34], free-radical scavenging [35-36], and many other pharmacological activities. Also, it has
118 been reported that MYR can easily pass through the blood-brain barrier [37].

119 In this study, we investigated the possible antioxidant effects of MYR toward EPX-induced
120 oxidative stress on F98 cells [3]. In particular, we showed its capacity to alleviate most, if not
121 all, the known EPX-induced cytotoxicity and apoptosis on this neural cell model.

122

123

124

125 **2. Materials and methods**

126 **2.1. Chemicals**

127 Epoxiconazole, Myricetin, Pyrogallol, N acetylcysteine and Hydrogen peroxide were
128 purchased from Sigma - Aldrich (St. Louis, MO, USA). 3-4,5-Dimethylthiazol-2-yl, 2,5-
129 Diphenyltetrazolium Bromide (MTT), Cell Culture Medium (DMEM), Fetal Calf Serum
130 (FCS), Phosphate Buffer Saline (PBS), Trypsin-EDTA, Penicillin and Streptomycin mixture
131 and L-Glutamine (200 mM) were bought from GIBCO-BCL (UK). 2,7-Dichlorofluoresce
132 Diacetate (DCFH-DA) was supplied by Molecular Probes (CergyPontoise, France). The Mito-
133 tracker Red CMXRos dyes were purchased from Invitrogen. All other chemicals used were
134 of analytical grade.

135 **2.2. Cell culture and treatment**

136 Rat F98 cells were cultured in DMEM, supplemented with 10 % FBS, 1 % L-Glutamine (200
137 mM), 1 % of mixture Penicillin (100 IU/ml), and Streptomycin (100 µg/ml), at 37 °C with 5
138 % CO₂ and 95 % O₂ as previously described [3]. The media was replaced by new medium on
139 alternate days and pre-treated with increasing concentrations of MYR (10, 20 and 50 µM)
140 during 2 hours before treatment with different concentrations of EPX dissolved in water and
141 DMSO (1:4, v:v). A negative control containing cells treated with vehicle (DMSO) was also
142 evaluated. The final DMSO concentration in the treated and control cultures does not exceed
143 0.1%. Positive controls treated with H₂O₂ (hydrogen peroxide at 20 µM) and NAC (N
144 acetylcysteine at 1mM) were added. Positive controls containing cells treated only with
145 increasing concentrations of MYR (10, 20 and 50 µM) was also presented in Fig. 2.

146 **2.3. Cell viability assay (MTT assay)**

147 Cell viability was quantitatively determined by 3-4,5-Dimethylthiazol-2-yl, 2,5-
148 Diphenyltetrazolium Bromide (MTT) assay [38]. F98 cells were grown in 96-well plates and
149 incubated at 37 °C for 24 h with EPX (50 µM, corresponding to the IC₅₀) and with increasing
150 concentrations of MYR (10, 20 and 50 µM) separately or with the combination of them (pre-
151 treatment with MYR two hours before adding EPX). The results were expressed as the
152 percentage of MTT reduction relative to the absorbance measured from negative control cells.

153 **2.4. Cell cycle analysis**

154 The F98 cells were grown in 6-well plates and treated with EPX (50 μ M) alone or with MYR
155 (10, 20, and 50 μ M) at 37 °C for 24 hours. As previously described by Hamdi et al. (2019),
156 F98 cells were harvested, washed with cold PBS, and processed for cell cycle analysis by
157 flow cytometry. The percentages of cell distribution in sub-G0/G1, G0/G1, S, and G2/M
158 phases were evaluated by using WinMDI 2.9 [39].

159 **2.5. ROS determination**

160 The conversion of non-fluorescent 2,7-dichlorofluorescein diacetate (DCFH-DA) to
161 fluorescent DCF was used extensively to monitor oxidation in biological systems detecting
162 and quantifying intracellular products such as Superoxide radicals, Hydroxyl radicals, and
163 Hydrogen peroxide [40-42]. F98 cells were grown in 96-well culture plates (Pollylabo, France)
164 and pre-treated with increasing concentrations of MYR (10, 20, and 50 μ M) during 2 hours
165 before treatment with EPX for 24 hours at 37 °C. Then, cells were incubated with 20 μ M of
166 cell-permeable DCFH-DA for 30 min, treated with EPX at 50 μ M and incubated for 24 hours
167 at 37 °C. The DCF fluorescence was measured using a fluorometer (Biotek FLx800) and the
168 amount of ROS produced was proportional to the DCF fluorescence.

169 **2.6. Protein extraction**

170 F98 Cells (10^6 cells/well) were seeded for 24 h in six-well multi-dishes (Pollylabo, France)
171 and incubated at 37 °C for 24 h with EPX alone or combined to MYR (10, 20 and
172 50 μ M). Cells were rinsed with ice-cold PBS, scraped, collected in a lysis buffer (Hepes 0.5 M
173 containing 0.5 % Nonidet-P40, 1 mM PMSF, 1 μ g/ml Aprotinin, 2 μ g/ml Leupeptin, pH 7.4),
174 and incubated for 20 min in ice before centrifugation. Protein concentration was determined
175 in cell lysates using the Protein Bio-Rad assay [43].

176 **2.7. Measurement of SOD activity**

177 Superoxide Dismutase (SOD) activity was determined according to the method described by
178 Marklund and Marklund [44] by assaying the auto-oxidation and illumination of Pyrogallol at
179 440 nm for three minutes. One unit of SOD activity was calculated as the amount of protein
180 that caused 50 % Pyrogallol auto-oxidation inhibition. The SOD activity is expressed as units
181 per milligram of protein.

182 **2.8. Measurement of Catalase (CAT)**

183 The CAT activity was measured according to the method described by Aebi (1984) [45]
184 assaying the hydrolysis of H₂O₂ and the resulting decrease of absorbance at 240 nm over a 3-
185 min period at 25 °C. The activity of CAT was calculated using the molar extinction
186 coefficient (0.04/mM/cm). The results were expressed as micromole per minute per milligram
187 of protein.

188 **2.9. Lipid peroxidation**

189 For the detection of lipid peroxidation, Malondialdehyde (MDA) product was measured. F98
190 cells were seeded and exposed to EPX alone or combined with MYR (10, 20, and 50µM) for
191 24 h at 37 °C. After treatment, the test was done according to the original procedure of
192 Ohkawa et al. (1979) [46], as described in detail by Hamdi et al. (2019). The concentration of
193 MDA was determined according to a standard curve.

194 **2.10. Immunocytochemistry analysis**

195 In order to view the effect of EPX and MYR on the cytoskeleton network,
196 immunocytochemistry assay was done. F98 cells were grown in 24-well plates containing
197 coverslips and exposed at 37 °C for 24 h to EPX alone or combined to MYR (10, 20, and
198 50µM). After the treatment period, the assay was performed according to the original
199 procedure of Balzeau et al. (2012) [47], as described in detail elsewhere [3]. Images were
200 taken with an Olympus Confocal Microscope (BX50) after incubation of cells with anti-
201 Alpha-Tubulin antibody or anti-mouse Vimentin antibody and revelation with an anti-mouse
202 Alexa antibody (568 nm).

203 **2.11. DNA damage assessed by the Comet assay**

204 For the detection of DNA damage, F98 cells were seeded in six-well culture plates (Pollylabo,
205 France) and exposed to EPX alone or were pre-treated with MYR during 2 hours before
206 treatment with EPX for 24 h at 37 °C. At the end of exposure period, the test was performed
207 according to the original method of Collins et al. (1996) [48], as described in detail elsewhere
208 [3]. One hundred cells were randomly selected and analyzed from each experimental point.
209 The percentage of DNA in the comet tail (ie, tail intensity %) was used as a measure of the
210 extent of DNA damage.

211 **2.12. Annexin V-FITC/PI double staining assay**

212 For the detection of apoptosis, F98 cells were grown in 6-well plates and treated with EPX
213 (50 μ M) and/ or MYR at the indicated concentrations for 24h. After the treatment, F98 cells
214 were harvested and analyzed for apoptosis by flow cytometry analysis after staining with
215 Annexin V FITC and Propidium Iodide (PI) [49].

216 **2.13. Mitochondrial Membrane Potential and Mito-tracker Assay**

217 For the estimation of mitochondrial membrane potential, the cationic fluorescent dye
218 Rhodamine-123 has been used. The F98 cells were grown in 96-well culture plates and treated
219 with EPX alone or combined to MYR for 24 h. At the end of treatment, the assay was done
220 according to the original method of Debbasch et al. (2001) [50], as described in detail by our
221 previous work [3]. The results were expressed as the percentage of absorbed Rhodamine-123
222 fluorescence relative to the fluorescence measured from negative control cells.

223 F98 cells were also seeded onto Ibidi 4 well slides and cultured for 24 h. After treatment with
224 EPX (50 μ M) and/or MYR (10, 20, and 50 μ M) for 6 hours, the cells were stained with the
225 Mito-tracker Red CMXRos according to the manufacturer's instructions and observed by
226 confocal microscopy.

227 **2.14. Caspases activation**

228 The evaluation of Caspase-3 and/or caspase-9 activity was performed using a commercially
229 available kit, according to the manufacturer's instructions (Promega, France), and according
230 to Rjiba-Touati et al. (2013) [51]. In the presence of active Caspase-3, cleavage and release of
231 pNA from the substrate occur. Free pNA produces a yellow color detected by a
232 spectrophotometer at 405 nm. A standard curve was realized in order to determine the
233 correspondence between optical density and pNA concentration.

234 **2.15. Statistical analysis**

235 Data are expressed as the mean \pm standard deviation (SD) of the means. The analysis
236 parameters were tested for homogeneity of variance and normality. The data were therefore
237 analyzed using a one-way analysis of variance (ANOVA) with a post hoc Tukey–Kramer test
238 to identify significance between groups and their respective controls. In all cases, $p < 0.05$ was
239 considered statistically significant.

240 **3. Results**

241 **3.1. Measurement of cell viability and proliferation**

242 F98 cells were exposed to increasing concentrations of EPX and MYR separately and to the
243 combination of the two products during 24 hours, and then their viability was determined by
244 MTT assay. The results indicate that EPX induced a dose-dependent decrease of cell viability
245 ($p < 0.05$) (Fig. 1A) and altered the cell morphology (Fig. 1B) as previously published [3].
246 The IC₅₀ value determined after 24 hours of cell treatment was about 50 μ M. In this study,
247 we used this value to investigate the possible effects of MYR.

248 While MYR alone exhibited no detectable toxicity towards F98 cells (Fig. 1A), pre-treatment
249 with this Flavonoid at 10, 20, and 50 μ M during 2 hours before treatment with EPX,
250 significantly decreased the EPX-mediated cytotoxicity (Fig. 1C) and restored normal cell
251 morphology (Fig. 1B). Indeed, cell viability was increased from $49 \pm 0.05\%$ in the presence of
252 EPX alone to $57.43 \pm 0.02\%$, $65.5 \pm 2.43\%$ and $75.6 \pm 0.05\%$, when cells were pre-treated
253 with MYR at respectively 10, 20 and 50 μ M, and during two hours before EPX treatment (Fig.
254 1C).

255 Then, to examine at which level of the cell cycle MYR protects cells from the cytotoxic effect
256 of EPX, we used flow cytometry to determine the effect of EPX alone (50 μ M) or following
257 the pre-treatment with MYR at these concentrations (10, 20 and 50 μ M). The cell cycle
258 analysis showed that F98 cells accumulated in the G₂/M phase with IC₅₀ of EPX (50 μ M),
259 with the inhibition of DNA synthesis at the S phase. Interestingly, the pre-treatment with
260 MYR reduced this effect in a dose-dependent manner (Fig. 1D).

261 **3.2. Myricetin inhibits Epoxiconazole-induced ROS generation**

262 The toxicity of EPX has been linked to the generation of oxidative stress in F98 cells [3].
263 Therefore, we evaluated whether MYR exerts its proposed antioxidant properties and
264 modulates the level of ROS induced by EPX. The level of intracellular ROS was measured by
265 recording the fluorescence of DCF, which is the result of DCFH oxidation mainly by H₂O₂.
266 As shown in Fig. 2A, the 50 μ M of EPX treatment induced a significant increase of ROS
267 production to about 3.50-fold when compared to untreated cells. Positive control treated with
268 H₂O₂ (20 μ M) also increased the ROS levels to 4.8-fold to untreated cells ($p < 0.001$).
269 Moreover, the pre-treatment with MYR during two hours at different doses (10, 20, or 50 μ M)

270 before the exposure to EPX significantly reduces the intracellular ROS generated by EPX. On
271 the other hand, in order to examine the role of ROS in the EPX-induced cell death, F98 cells
272 were pre-treated for 2 h with the N-acetylcysteine (NAC) at 1mM before exposure to EPX for
273 24h. Our results showed that NAC pre-treatment strongly abolishes the ROS generation
274 induced by EPX.

275 **3.3. Effect of Myricetin on Epoxiconazole-induced Lipid peroxidation**

276 As an index of lipid peroxidation, the intracellular concentration of MDA was measured in
277 F98 cells. As shown in Fig. 2B, the EPX treatment (50 μ M) provoked a strong increase in the
278 intracellular concentration of MDA (3.5 ± 0.08 μ mol/mg protein), versus (0.5 ± 0.06 μ mol/mg
279 protein) for untreated cells, which indicates an important oxidative insult to cell lipids.
280 Positive control treated with H₂O₂ (20 μ M) increased the MDA level to 5.1 ± 0.02 μ mol
281 MDA/mg of protein ($p < 0.001$). However, pre-treatment of cells with MYR significantly
282 reduced the level of lipid peroxidation induced by EPX. In fact, the MDA level reached $2.1 \pm$
283 0.07 , 1.5 ± 0.08 and 0.9 ± 0.04 μ mol/mg protein following MYR pre-incubation at
284 respectively 10, 20 and 50 μ M. The pretreatment with NAC at 1mM 2 hours before EPX
285 exposure significantly reduced the level of lipid peroxidation induced by EPX.

286 **3.4. Myricetin modulates Antioxidant Enzyme activities following Epoxiconazole** 287 **treatment**

288 Changes in the levels of antioxidant enzyme activity represent a sensitive biomarker of the
289 cellular response. SOD catalyzes the dismutation of the highly reactive superoxide anion from
290 oxidative stress to H₂O₂, which can further be decomposed to water and oxygen by CAT or
291 GPx. To characterize the possible protective effects exerted by pre-treatment with MYR, we
292 measured changes in the activities of intracellular antioxidant enzymes (Fig. 2C-D).
293 Treatment of F98 cells with 50 μ M EPX induced significant increases in the enzyme
294 activities. The CAT activity increased from 5 ± 0.1 μ mol/min/mg of protein in untreated cells
295 to 40 ± 0.6 μ mol/min/mg of protein in the presence of 50 μ M EPX (Fig. 2C), and SOD
296 activity raised from 4 ± 0.1 USOD/min/mg of protein in control cells to 23 ± 0.5
297 USOD/min/mg of protein in the presence 50 μ M EPX (Fig. 2D). The treatment of F98 cells
298 with H₂O₂ (20 μ M) (positive control) strongly increased the antioxidant enzymes activities.
299 However, the two hours pre-treatment with MYR (10, 20 and 50 μ M) before adding EPX

300 significantly reduced these increases in a dose-dependent manner (Fig. 2C-D). Indeed, the
301 pretreatment with NAC significantly decreased the activity of these antioxidant enzymes.

302 **3.5. Myricetin reduces the Epoxiconazole-induced Cytoskeleton disruption and DNA** 303 **fragmentation**

304 We next evaluated the ability of MYR to modulate the EPX induced DNA fragmentation and
305 cytoskeleton disruption, two apoptotic hallmarks. DNA damages were analyzed using the
306 alkaline Comet assay. The high sensitivity of the Comet assay allows measurement of DNA
307 fragmentation in individual cells. As shown in Fig. 3A, induced 250 ± 4.2 of total score of
308 DNA damage at concentration of IC₅₀ (50 μ M), as compared to 30 ± 4.48 of the score in
309 control cells (untreated cells). The addition of MYR significantly decreased the DNA
310 fragmentation induced by EPX that reached 90.1 ± 6.2 for 50 μ M of MYR (Fig. 3A).

311 The effects of the EPX in the presence or absence of MYR on the different cytoskeleton
312 structures in F98 cells are shown in Fig.4. In the control group, the cells exhibited a normal
313 and characteristic network of microtubules (MTs) (Fig. 4A), and intermediate filaments (IFs)
314 (Fig. 4B). On the opposite, in the cells treated with 50 μ M EPX, the cell boundaries were
315 unclear, and the networks of microtubules and intermediate filaments were strongly altered or
316 even lost in multiple cells. Interestingly, the pre-treatment with MYR at different
317 concentrations (10, 20, and 50 μ M) protected the cytoskeleton from a disruption in a dose-
318 dependent manner (Fig. 4A & 4B). Together, these data demonstrated that MYR protects cells
319 from the EPX-induced DNA fragmentation and cytoskeleton disruptions.

320 **3.6. Effect of Myricetin on Epoxiconazole-induced Apoptosis**

321 We have previously reported that EPX induces cell death by activating the intrinsic apoptotic
322 pathway (Hamdi et al., 2019). We thus assessed the possible effect of MYR on the
323 mitochondrial alterations induced by EPX. To this end, cells were stained with Rhodamine
324 123 (Rh123) to measure the mitochondrial transmembrane potential ($\Delta\Psi_m$).

325 As shown in Fig. 3F, the EPX treatment reduced the Rh-123 uptake to $49 \pm 1.1\%$, indicating a
326 loss of mitochondrial potential. However, the pre-treatment of cells by MYR restored the
327 percentage of Rh123 uptake in a dose-dependent manner: $62 \pm 2.1\%$, $70 \pm 2.3\%$ and $82 \pm$
328 1.2% for respectively MYR at 10, 20 and 50 μ M. These results indicate that MYR reduces the
329 mitochondrial alterations induced by EPX.

330 To visualize the structural abnormalities of mitochondria following EPX and/or MYR
331 exposure, we performed a detailed confocal microscopic analysis using a cell-permeable
332 mitochondria selective dye MitoTracker CMXRos Red, which passively diffuses across the
333 plasma cell membrane and accumulates in active mitochondria of F98 cells. Mitochondria
334 from control cells appear as long, thread-like structures that were well linked and randomly
335 distributed throughout the cells. Disruption of the tubular mitochondria network and
336 formation of punctuating staining were observed in EPX-treated F98 cells, indicating
337 fragmentation of mitochondria due to oxidative stress (Fig. 4D).

338 On the contrary, no fragmentation of mitochondria was observed in EPX+ MYR-treated cells;
339 in fact, MYR-treated cells maintained the normal tubular morphology (Fig. 4D). These results
340 indicate that MYR prevents mitochondria damage induced by oxidative stress in F98 cells.

341 Besides, the double staining of cells with FITC-labeled-Annexin V and PI allowed to confirm
342 by flow cytometry that EPX induced apoptosis. Compared to the control values, the 50 μ M
343 EPX treatment increased the percentage of early and late apoptotic cells. The rate of apoptosis
344 is the sum of early and late apoptotic cells. We have added in Fig. S2 representative
345 cytograms with quadrant analysis of the time course of EPX treatment to show that late
346 apoptotic cells actually derive from early ones. Nevertheless, when cells were pre-treated with
347 MYR for two hours before treatment with EPX, it significantly reduced the rate of apoptotic
348 cells (Fig. 3E).

349 When the cells prepare to die with programmed cell death, several morphological changes are
350 produced, like a condensation of chromatin into sharply delineated masses and DNA
351 fragmentation, followed by degradation of nuclei into discrete particles [52-53]. DAPI
352 staining and flow cytometric DNA analysis of sub-G0/G1 peak showed that EPX treatment at
353 50 μ M for 24 h induced the condensation of chromatin and the fragmentation of nuclei
354 respectively. However, the pre-treatment with MYR at different doses abolished these effects
355 (Fig. 4C, Fig. S1 and Fig. S3).

356 In order to confirm the possible implication of caspases in the process of apoptotic death, we
357 added the caspase inhibitor Z-vad-fmk (50 μ M) during 2 h before treating F98 cells by EPX.
358 Such a pretreatment with Z-vad-fmk induced a significant inhibition of cell mortality ($P <$
359 0.05). On the other hand, pretreatment with MYR before adding Z-vad-fmk for 2 hours
360 strongly induced an increase of cell viability.

361 As illustrated in Fig. 3B, a significant ($p < 0.05$) increase in Caspase-3 activity was observed
362 in F98 cells treated with EPX alone as compared to untreated cells (3 ± 0.1 pmolpNA/h/mg of
363 protein vs. 19 ± 0.5 pmolpNA/h/mg of protein). This activity decreased significantly in the
364 presence of MYR pre-treatments: respectively 14 ± 0.04 ; 10.1 ± 0.01 and 8.3 ± 0.02
365 pmolpNA/h/mg of protein at 10, 20, and 50 μ M.

366 Apoptosis can be triggered either by an external death receptor stimulus (extrinsic) or through
367 internal (intrinsic) mitochondria-mediated signaling. In order to confirm the intrinsic
368 apoptotic pathway induced by EPX, specific inhibitor of caspase-9 Z-LEHD-FMK (20 μ M)
369 was added during 2 h before treating F98 cells by EPX. The pretreatment with Z-LEHD-FMK
370 induced a significant inhibition of apoptosis rate ($P < 0.05$). However, pretreatment with
371 MYR before adding Z-LEHD-FMK for 2 hours strongly induced a decrease of apoptosis rate.

372 As presented in Fig. 3D, a significant ($p < 0.05$) increase in Caspase 9 activity was observed
373 in F98 cells treated with EPX alone as compared to untreated cells (5.6 ± 0.03 pmolpNA/h/mg
374 of protein vs. 0.9 ± 0.05 pmolpNA/h/mg of protein). This activity decreased significantly in
375 the presence of MYR pre-treatments: respectively 4.8 ± 0.03 ; 3.3 ± 0.02 and $2.6 \pm$
376 0.05 pmolpNA/h/mg of protein at 10, 20, and 50 μ M.

377

378

379

380

381

382 **4. Discussion**

383 Due to their very high use in agriculture, pesticides are widely disseminated in the
384 environment. Increased exposure to pesticide residues poses a serious risk to human health.
385 The great interest of the scientific community is mainly focused on Triazole fungicides, one
386 of the most economical molecules from the fungicide family [54]. Amongst these products,
387 Epoxiconazole is a particularly persistent pollutant with harmful effects on both animals and
388 humans [55]. Increasing evidence indicates that EPX accumulates in the nervous system and
389 induces neurodegeneration [1]. Previous studies showed that the exposure to pesticides
390 induces an imbalance in the redox status within the cells followed by their programmed cell
391 death [3]. As Epoxiconazole is a liposoluble compound, it can easily cross the blood-brain
392 barrier, which makes it frequently exposed to repeated doses of EPX by drinking and
393 ingesting contaminated water and food like fishes [56]. Besides, the acceptable daily intake
394 (ADI) (is an estimate of the amount of a substance in food or drinking water that can be
395 consumed daily over a lifetime without presenting an appreciable risk to health) of EPX was
396 estimated by the EFSA (2008) to 8µg/kg [57]. On the other hand, the determined IC50 (15
397 µg/ml) on F98 cells seems to be not much higher (1.8 fold) than the daily intake of EPX.
398 Moreover, neurodegenerative disorders are associated with high morbidity and mortality, and
399 few effective options are available for their treatment [58]. Therefore, many studies have been
400 conducted focusing on natural compounds present in food as important molecules against
401 neurodegenerative diseases such as Parkinson's disease [59-62]. Natural polyphenols exert
402 numerous biological activities, like antioxidant, anti-inflammatory, antiviral, antibacterial,
403 antiproliferative, and anticarcinogenic capacities [63], as well as cellular redox state
404 modulation activities through direct action on enzymes, proteins and receptors [64-65].
405 Myricetin is one of the key constituents of various human foods and beverages including
406 vegetables, teas and fruits, and is recognised mainly for its iron-chelating, anti-oxidant, anti-
407 inflammatory and anticancer properties. It displays several activities that are related to the
408 central nervous system and numerous studies have suggested that these compounds may be
409 beneficial to protect against diseases such as Parkinson's and Alzheimer's [66]. Glial cells
410 represent the first target of oxidative stress in the nervous system, and various natural
411 antioxidants have been described to prevent functional damage of these cells by oxidative
412 stress [67]. Accumulating data proved the strong antioxidant properties of Myricetin (MYR)
413 in various cell models, but it has not yet been evaluated in glial cells. Our study investigates
414 the protective effects and mechanisms of MYR in the prevention of ROS generation and
415 programmed cell death induced by EPX using F98 cell model. As previously shown, we used

416 F98 cells because of their large size necessary to elucidate more precisely the effects of EPX
417 on organelles, in particular the cytoskeleton and mitochondria. Moreover, their high capacity
418 for proliferation allows the careful characterization of their different cellular pathways. The
419 ability to sense oxidative and proteotoxic insults and to coordinate defensive stress response
420 are basic elements for cellular adaptation and survival [68-69]. In this regard, plant
421 polyphenols are produced by plants to defend themselves against pests such as bacteria, fungi,
422 and insects, to which they are toxic. One possible mode of action of natural polyphenols is the
423 hormesis effect [70]. Consistently, hormesis dose response is characterized by low dose
424 stimulation and a high dose inhibition. The biphasic dose-response phenomenon is
425 characterized by a U-shaped or inverse dose response curve, depending on the different
426 measured endpoints [71-73]. The biological processes underlying hormetic dose-response,
427 recently focused attention in the field of neuroprotection, which was mainly elucidated
428 through the exploitation of bioactive polyphenols with the result of activating various cell
429 defense systems aimed at controlling the redox environment, the proteostatic and metabolic
430 homeostasis, organelle turnover, the inflammatory response, and others, thus making cells
431 more resistant to subsequent toxic stimuli, particularly in aged people [74-75]. The
432 polyphenolic compounds such as flavonoids have been commonly used in the human diet.
433 They are known to restore DNA damage and repair, cell cycle, and apoptosis-related multiple
434 cellular signaling pathways [2]. The protective effects of MYR, a potent antioxidant Flavonol,
435 have been studied in several studies against ROS production-induced injuries [76]. Several
436 studies showed the neuroprotective effects of MYR. It has been shown that MYR protects
437 against rotenone-induced cytotoxicity in SH-SY5Y cells [77], MYR also inhibits the
438 formation and extension of β -amyloid protein for the prevention of Alzheimer's disease [78],
439 and the 6-hydroxydopamine which induce neurotoxicity in rats [79]. Moreover, previous
440 findings support that MYR induces an anti-apoptotic activity as described by Shimmyo et al.
441 (2008) [80] who demonstrated that MYR alleviated beta-amyloid (A β)-induced apoptosis
442 in Alzheimer's Disease (AD) brain of the rat by the inhibition of chromatin condensation and
443 caspases-3 activity. To our knowledge, these protective effects of MYR are attributed to its
444 antioxidant properties and the protective effect against mitochondrial failure [81].

445 In this study, the pre-treatment of MYR increased in a dose-dependent manner the viability
446 and the proliferation of EPX-treated F98 glial cells concomitant with a proportional decline in
447 their reactive oxygen species (ROS) generation. These results are in line with the study of
448 Molina-Jimenez. (2003), demonstrating that MYR suppressed the production of ROS [82]. In

449 addition, we also found that MYR pre-treatment inhibits EPX-induced lipid peroxidation and
450 DNA damage, and decreases cytoskeleton disruption in F98 cells. Our results are in
451 accordance with the finding of Wang and al. (2010) which proved the efficiency of MYR to
452 prevent H₂O₂-induced DNA damage and lipid peroxidation in Chinese Hamster Lung
453 Fibroblasts (V79-4) cells [83]. During the development of oxidative stress, the organism will
454 trigger enzymatic/nonenzymatic antioxidant mechanisms to protect the cells against oxidative
455 damage. SOD and CAT are the first line of defense against oxidative damage [84]. MYR
456 significantly decreased the activities of these enzymes. Novel data presented the involvement
457 of Nrf2, a vital defender of the anti-oxidative regulation system in MYR-mediated
458 neuroprotection and function recovery [85]. Emerging research has recently focused on
459 biological relevance for cell protection in many degenerative diseases and for neuroprotection
460 in several neurodegenerative disorders, particularly Alzheimer disease and Parkinson disease,
461 of the redox homeostasis elicited by plant polyphenols through the activation of vitagene
462 signaling pathways. The latter involves redox sensitive genes such as the Hsp70, heme-
463 oxygenase-1 (HO-1), thioredoxin/thioredoxin reductase, and sirtuins system. Gene expression
464 of these cytoprotective proteins is coordinately regulated by a common molecular mechanism
465 that involves the Nrf-2 Kelch-like ECH-associated protein 1 (KEAP1)-dependent signal
466 pathways. An essential feature of the stress response initiated by electrophilic species is the
467 nuclear localization of the transcription factor Nrf2 (NF-E2 related factor 2) and the
468 subsequent binding of Nrf2 to a DNA recognition sequence known as antioxidant response
469 element (ARE) or electrophile response element (EpRE), defined phase 2 response. Nrf2 is a
470 key transcription effector for the activation of wide range of cytoprotective genes (>500). The
471 Nrf2 activity induces a mild stress response, providing a healthy physiological steady state
472 and extending lifespan in different cells and animal models. Chemicals that stimulate the
473 nuclear accumulation of Nrf2, thereby enhancing the expression of phase 2 detoxification
474 enzymes. Under basal conditions the pathway operates at low levels due to the repressor
475 function of the cytosolic protein Keap1, which binds to the E3 ubiquitin ligase Cullin3-RING
476 box1 and presents Nrf2 for ubiquitination and subsequent proteosomal degradation. Indeed,
477 there is now compelling experimental evidence that exogenous and endogenous inducers
478 chemically modify specific and highly reactive cysteine residues of Keap1, which, in addition
479 to being a repressor for Nrf2, also functions as the intracellular sensor for inducers. This
480 reaction leads to conformational changes in Keap1 that abrogate its ability to repress Nrf2,
481 ultimately resulting in Nrf2 stabilization, binding to the ARE and recruitment, the basal
482 transcriptional machinery to activate transcription of cytoprotective genes. On the other hand,

483 a chronic long-term Nrf2 stimulation may lead to pathophysiological events, therefore the
484 Nrf2 signaling can be considered as a hormetic-like pathway. Increasing evidences show that
485 plant polyphenols activate the phase 2 response leading to the expression of various Nrf2-
486 dependent antioxidant vitagenes. These effects represent a powerful instrument supporting
487 redox homeostasis under stressful conditions and support the assumptions that the helpful
488 properties of polyphenols carry out through adaptive stress response vitagenes. Currently,
489 increasing evidence suggests that plant polyphenols may offer beneficial effects acting in a
490 hormetic-like manner by activating adaptive stress-response pathways and making the
491 hormesis concept fully applicable to the field of nutrition. Moreover, it has been considered
492 that plant polyphenols may be protective through hormetic processes that involve the stress-
493 activated “vitagenes” [74], [86-92].

494 Mitochondria represent the major source and target of oxidative stress. Previous finding
495 proved that the production of ROS had been involved in the disturbance of mitochondrial
496 forms and functions [93]. Our results show that MYR treatment recovered the damaged
497 mitochondria post oxidative stress, as evident by regaining the tubular filamentous
498 mitochondrial morphology in F98 cells. Moreover, apoptosis can be categorized into two
499 pathways, generally mitochondria-dependent intrinsic and death receptor-mediated extrinsic
500 apoptotic signaling pathways. Although previous research has extensively implicated the
501 importance of mitochondria in the pathogenesis of stroke, the excessive ROS generation in
502 EPX-treated F98 cells induces the loss of mitochondrial membrane potential, which is
503 considered to be a characteristic of the onset of the intrinsic apoptotic pathway [94-95]. Pre-
504 treatment of MYR was also effective in inhibiting the mitochondrial-mediated apoptosis
505 induced by EPX in F98 cells. In accordance with our findings, Wu et al., (2016) demonstrated
506 that MYR improves mitochondrial function in the ischemic cerebrum, as indicated by the
507 recovered mitochondrial membrane potential ($\Delta\psi$) [96]. In addition, Zou et al., (2015)
508 revealed that MYR counteracts the mitochondrial dysfunction, which is mainly attributed to
509 its role in the induction of mitochondrial biogenesis by the activation of AMP-activated
510 protein kinase (AMPK) followed by the activation of the peroxisome proliferator-activated
511 receptor gamma coactivator-1-alpha (PGC-1 α), a master regulator of mitochondrial
512 biogenesis during acute hypoxia in rats [97]. When cells are subjected to a variety of
513 oxidative environmental stresses, they typically respond by inducing phase II detoxifying
514 enzymes and by stimulating mitochondrial biogenesis, two of the most important pathways
515 for cells to react against oxidative stress. Nrf2 controls the orchestrated expression of phase II

516 enzymes and genes involved in oxidative defense. The increase in nuclear Nrf2 level should
517 be the key index of the activation of the phase II detoxifying enzymes including γ -glutamyl-
518 cysteinyl-ligase, NADPH (nicotinamide adenine dinucleotide phosphate)-quinone-
519 oxidoreductase 1, heme-oxygenase-1, superoxide dismutase, peroxiredoxin and thioredoxin as
520 well as other antioxidant enzymes [98-100]. Moreover, Phase II enzymes perform a variety of
521 vital cellular functions important for protecting against oxidative damage. On the other hand,
522 the stimulation of mitochondrial biogenesis is important as an adaptive mechanism in the
523 cellular response to different stressors. Mitochondrial biogenesis also seems to be a promising
524 therapeutic target as it provides a protective mechanism in a broad spectrum of acute and
525 chronic diseases manifested by mitochondrial dysfunction [101]. This may be achieved by
526 activation of the key factor promoting mitochondrial biogenesis, peroxisome proliferator-
527 activated receptor coactivator 1 alpha (PPARGC1 α) [26]. PPARGC1 α is a co-transcriptional
528 regulation factor that regulates the process of mitochondrial biogenesis by interacting with
529 many transcription factors/proteins such as nuclear respiratory factors (NRF-1 and NRF-2),
530 mitochondrial transcription factor A (Tfam), uncoupling proteins (UCP2) [102-104]. NRF-1,
531 NRF-2, and Tfam regulate the transcription of genes encoding respiratory complex subunits
532 and mtDNA synthesis [105].

533 Furthermore, Caspase-3 is considered the key effector of Caspases, involved in both intrinsic
534 and extrinsic apoptotic pathways that will be activated in response to cytotoxic drugs [106].
535 The exposure to EPX induced a significant increase in the activity of Caspase-3 of F98 cells.
536 Nevertheless, pre-treatment with MYR alleviates the Caspase-3 induction. The protective
537 action of MYR may be due to its direct inhibition of the active site of Caspase-3 and thus
538 reducing directly Caspase-3 activity [80]. Indeed, Caspase-9 is a key player in the intrinsic or
539 mitochondrial pathway. The EPX treatment significantly increased the activity of Caspase-9
540 of F98 cells. However, pre-treatment with MYR strongly reduced this increase.

541 Our results suggest that the underlying mechanism of the protective action of MYR against
542 EPX-induced toxicity probably operates through the free radical scavenging activity of MYR.
543 The ability of MYR to boost up the cellular antioxidant defense system can be explained by
544 the following mechanisms: one possible underlying mechanism may involve its catechol-like
545 structure since it is known that catechol-containing polyphenols are potent radical scavengers
546 and chelators of ferric ion [107-108]. In addition, the antioxidant activity of MYR could also
547 operate through oxidation of the three hydroxyl groups (3',4',5'-position) attached in its B-ring
548 [109].

549 In conclusion, our findings showed for the first time that MYR, the common antioxidant food
550 component, protects F98 cells from EPX by inhibiting oxidative stress upstream event, which
551 then leads to DNA damage, cytoskeleton disruption, and apoptotic cell death. These results
552 indicate that the use of MYR as a dietary supplement might be helpful to prevent EPX-related
553 neurotoxicity.

554

555

556

557

558

559

560

561

562 **Conflict of interest**

563 The authors declare that there is no conflict of interest.

564 **Acknowledgements**

565 This work is supported by INSERM (Institut National de la Santé et de la Recherche
566 Médicale) and the Ligue contre le Cancer to Joel EYER.

567

568 **5. References**

- 569 [1] Heusinkveld, H. J., Molendijk, J., van den Berg, M., and Westerink, R. H. S. 2013. Azole
570 Fungicides Disturb Intracellular Ca^{2+} in an Additive Manner in Dopaminergic PC12
571 Cells. *Toxicological Sciences*. 134, 374–381.
- 572 [2] Tiwari, P., and Mishra, K. P. 2019. Flavonoids sensitize tumor cells to radiation:
573 Molecular mechanisms and relevance to cancer radiotherapy. *International Journal of*
574 *Radiation Biology*. 1–39.
- 575 [3] Hamdi, H., Abid-Essefi, S., and Eyer, J. 2019. Cytotoxic and genotoxic effects of
576 epoxiconazole on F98 glioma cells. *Chemosphere*. 229, 314–323.
- 577 [4] Ramwell, C.T., Johnson, P.D, Boxall, ABA et al. 2004. Pesticide residues on the external
578 surfaces of field crop sprayers: environmental impact. *Pest Management Science*. 60,
579 795–802.
- 580 [5] Hamilton, A. J., Basset, Y., Benke, K. K., Grimbacher, P. S., Miller, S. E., Novotný, V.,
581 Yen, J. D. L. 2010. Quantifying Uncertainty in Estimation of Tropical Arthropod
582 Species Richness. *The American Naturalist*. 176, 90–95.
- 583 [6] Castelli, M.V., Butassi, E., Monteiro, M.C., Svetaz, L.A., Vicente, F., and Zacchino, S.A.
584 2014. Novel antifungal agents: a patent review (2011 - present). *Expert Opinion on*
585 *Therapeutic Patents*. 24, 323–338.
- 586 [7] Chen, Z.F., and Ying, G.G. 2015. Occurrence, fate and ecological risk of five typical azole
587 fungicides as therapeutic and personal care products in the environment: A
588 review. *Environment International*. 84, 142–53.
- 589 [8] Zarn, J.A., Bruschiweiler, B.J., Schlatter, J.R. 2003. Azole fungicides affect mammalian
590 steroidogenesis by inhibiting sterol 14 alpha-demethylase and aromatase. *Environ.*
591 *Health Perspect*. 111, 255–261.
- 592 [9] Kahle, M., Buerge, I.J., Hauser, A., Müller, M.D., and Poiger, T. 2008. Azole fungicides:
593 occurrence and fate in wastewater and surface waters. *Environmental Science and*
594 *Technology*. 42, 7193–200.
- 595 [10] Li, Y.B., Dong, F.S., Liu, X.G., Xu, J., Han, Y.T., and Zheng, Y.Q. 2014. Chiral
596 fungicide triadimefon and triadimenol: Stereoselective transformation in greenhouse
597 crops and soil, and toxicity to *Daphnia magna*. *Journal of Hazardous Materials*. 265, 115–
598 123.
- 599 [11] Zhang, Z., Jiang, W., Jian, Q., Song, W., Zheng, Z., Wang, D., and Liu, X.
600 2015. Residues and dissipation kinetics of triazole fungicides difenoconazole and
601 propiconazole in wheat and soil in Chinese fields. *Food Chemistry*. 168, 396–403.
- 602 [12] Moser, V. C. 2001. The Effects of Perinatal Tebuconazole Exposure on Adult
603 Neurological, Immunological, and Reproductive Function in Rats. *Toxicological*
604 *Sciences*, 62, 339–352.
- 605 [13] Chaâbane, M., Ghorbel, I., Elwej, A., Mnif, H., Boudawara, T., Chaâbouni, S. E.,
606 Soudani, N. 2016. Penconazole alters redox status, cholinergic function, and membrane-
607 bound ATPases in the cerebrum and cerebellum of adult rats. *Human and Experimental*
608 *Toxicology*. 36, 854–866.
- 609 [14] Chambers, J.E., Greim, H., Kendall, R.J, Segner, H., Sharpe, R.M., van der Kraak, G.
610 2014. Human and ecological risk assessment of a crop protection chemical: a case study
611 with the azole fungicide epoxiconazole. *Critical Reviews in Toxicology*. 44, 176–210.
- 612 [15] University of Hertfordshire. 2020. PPDB: Pesticide Properties DataBase.
- 613 [16] Hvězdová, M., Kosubová, P., Košíková, M., Scherr, K.E., Šimek, Z., Brodský, L.,
614 Šudoma, M., Škulcová, L., Sáníka, M., Svobodová, M., Krkošková, L., Vašíčková, J.,
615 Neuwirthová, N., 482 Bielská, L., Hofman, J. 2018. Currently and recently used

- pesticides in Central European arable soils. *Science of Total Environment*. 1, 613–614: 361–370.
- [17] Székács, A., Mörtl, M., Darvas, B. 2015. Monitoring pesticide residues in surface and ground water in Hungary: Surveys in 1990-2015. *Journal of Chemistry*. 1-15.
- [18] Vidal, J.L.M., Sánchez, J.A.P., Plaza-Bolaños, P., Frenich, A.G., Romero-González, R. 2010. Use of pressurized liquid extraction for the simultaneous analysis of 28 polar and 94 non-polar pesticides in agricultural soils by GC/QqQ-MS/MS and UPLC/QqQ-MS/MS. *Journal Of Aoac International*. 93, 1715–1731.
- [19] Bromilow, R.H., Evans, A.A., & Nicholls, P.H. 1999. Factors affecting degradation rates of five triazole fungicides in two soil types: 1. Laboratory incubations. *Pesticide Science*. 55, 1129–1134.
- [20] Kaziem, A.E., Gao, B., Li, L., Zhang, Z., He, Z., Wen, Y., & Wang, M. 2019. Enantioselective Bioactivity, Toxicity, and Degradation in Different Environmental Mediums of Chiral Fungicide Epoxiconazole. *Journal of Hazardous Materials*. 386, 121951.
- [21] Xiaotian, L.V., Chen, L.I.U., Yaobin, L.I., Yongxin, G.A.O., Jianzhong, L.I., Baoyuan, G.U.A.O. 2014. Stereoselectivity in bioaccumulation and excretion of epoxiconazole by mealworm beetle (*Tenebrio molitor*) larvae. *Environmental Safety*. 107, 71–76.
- [22] Kahle, M., Buerge, I. J., Hauser, A., Müller, M. D., & Poiger, T. 2008. Azole Fungicides: Occurrence and Fate in Wastewater and Surface Waters. *Environmental Science & Technology*. 42, 7193–7200.
- [23] Mendez, A., Castillo, L. E., Ruepert, C., Hungerbuehler, K., & Ng, C. A. 2018. Tracking pesticide fate in conventional banana cultivation in Costa Rica: A disconnect between protecting ecosystems and consumer health. *Science of The Total Environment*. 613-614:1250–1262.
- [24] Casado, J., Brigden, K., Santillo, D., & Johnston, P. 2019. Screening of pesticides and veterinary drugs in small streams in the European Union by liquid chromatography high resolution mass spectrometry. *Science of The Total Environment*. 670, 1204-1225.
- [25] Silva, V., Mol, H. G. J., Zomer, P., Tienstra, M., Ritsema, C. J., & Geissen, V. 2018. Pesticide residues in European agricultural soils – A hidden reality unfolded. *Science of The Total Environment*. 653, 1532-1545.
- [26] Petricca, S., Flati, V., Celenza, G., Di Gregorio, J., Lizzi, A. R., Luzi, C., Iorio, R. 2019. Tebuconazole and Econazole act synergistically in mediating mitochondrial stress, energy imbalance and sequential activation of autophagy and apoptosis in mouse Sertoli TM4 cells: possible role of AMPK/ULK1 axis. *Toxicological Sciences*.
- [27] Foley, P., Riederer, P., 2000. Influence of neurotoxins and oxidative stress on the onset and progression of Parkinson's disease. *Journal of Neurology*. 247, 82–94.
- [28] Sak K. 2014. Cytotoxicity of dietary flavonoids on different human cancer types. *Pharmacognosy Reviews*. 8, 122–146.
- [29] Chobot, V., Hadacek, F. 2011. Exploration of pro-oxidant and antioxidant activities of the flavonoid myricetin. *Redox Report*. 16, 242–247.
- [30] Phillips, P.A., Sangwan, V., Borja-Cacho, D., Dudeja, V., Vickers, S.M., Saluja, A.K. 2011. Myricetin induces pancreatic cancer cell death via the induction of apoptosis and inhibition of the phosphatidylinositol 3-kinase (PI3K) signaling pathway. *Cancer Letters*. 308, 181– 188.
- [31] Sun, F., Zheng, X.Y., Ye, J., Wu, T.T., Wang, J., Chen, W. 2012. Potential anticancer activity of myricetin in human T24 bladder cancer cells both in vitro and in vivo. *Nutrition and Cancer*. 64, 599–606.

- 664 [32] Shiomi, K., Kuriyama, I., Yoshida, H., Mizushina, Y. 2013. Inhibitory effects of
665 myricetin on mammalian DNA polymerase, topoisomerase and human cancer cell
666 proliferation. *Food Chemistry*.139, 910–918.
- 667 [33] Kim, M.E., Ha, T.K., Yoon, J.H., Lee, J.S. 2014. Myricetin induces cell death of human
668 colon cancer cells via BAX/BCL2-dependent pathway. *Anticancer Research*.34, 701–
669 706.
- 670 [34] Zhang, S., Wang, L., Liu, H., Zhao, G., Ming, L. 2014. Enhancement of recombinant
671 myricetin on the radiosensitivity of lung cancer A549 and H1299 cells. *Diagnostic*
672 *Pathology*. 9-68.
- 673 [35] Chen, W., Li, Y., Li, J., Han, Q., Ye, L., Li, A. 2011. Myricetin affords protection against
674 peroxynitrite-mediated DNA damage and hydroxyl radical formation. *Food and*
675 *Chemical Toxicology*. 49, 2439–2444.
- 676 [36] Krych, J., Gebicka, L. 2013. Catalase is inhibited by flavonoids. *International Journal of*
677 *Biological Macromolecules*. 58, 148–153.
- 678 [37] Wang, G., Wang, J. J., Tang, X. J., Du, L., & Li, F. 2016. In vitro and in vivo evaluation
679 of functionalized chitosan-Pluronic micelles loaded with myricetin on glioblastoma
680 cancer. *Nanomedicine*. 12, 1263–1278.
- 681 [38] Mosman, T. 1983. Rapid colorimetric assay for cellular growth and survival. Application
682 to proliferation and cytotoxicity assays. *Journal of Immunological Methods*. 65, 55–63.
- 683 [39] Mirza, M.B., Elkady, A.I., Al-Attar, A.M., Syed, F.Q., Mohammed, F.A., Hakeem, K.R.
684 2018. Induction of apoptosis and cell cycle arrest by ethyl acetate fraction of *Phoenix*
685 *dactylifera L.* (Ajwadates) in prostate cancer cells. *Journal of Ethnopharmacology*. 218,
686 35-44.
- 687 [40] Cathcart, R., Schwiers, E., Ames, B.N. 1983. Detection of picomole levels of
688 hydroperoxides using a fluorescent dichlorofluorescein assay. *Analytical Biochemistry*.
689 134, 111-116.
- 690 [41] Gomes, A., Fernandes, E., Lima, J.L. 2005. Fluorescence probes used for detection of
691 reactive oxygen species. *Journal of Biochemical and Biophysical Methods*.65, 45-80.
- 692 [42] Chen, T., Wong, Y.S. 2009. Selenocystine induces caspase-independent apoptosis in
693 MCF-7 human breast carcinoma cells with involvement of p53 phosphorylation and
694 reactive oxygen species generation. *The International Journal of Biochemistry and Cell*
695 *Biology*. 41, 666–676.
- 696 [43] Bradford, M.M. 1976. A rapid and sensitive method for the quantification of microgram
697 quantities of protein utilizing the principle of protein-dye binding. *Analytical*
698 *Biochemistry*. 72, 248–254.
- 699 [44] Marklund, S., Marklund, G. 1974. Involvement of the superoxide anion radical in the
700 autoxidation of pyrogallol and a convenient assay for superoxide dismutase. *European*
701 *Journal of Biochemistry*. 47, 469–474.
- 702 [45] Aebi, H. 1984. Catalase in vitro. *Methods in Enzymology*. 105, 121–126.
- 703 [46] Ohkawa, H., Ohishi, N., Yagi, K., 1979. Assay for lipid peroxide in animal tissues by
704 thiobarbituric acid reaction. *Analytical Biochemistry*. 95, 351-358.
- 705 [47] Balzeau, J., Peterson, A., Eyer, E. 2012. The vimentin-tubulin binding site peptide (Vim-
706 TBS.58-81) crosses the plasma membrane and enters the nuclei of human glioma cells.
707 *International Journal of Pharmaceutics*.423, 77-83.
- 708 [48] Collins, A.R., Dusinska, M., Gedik, C.M., Stetina, R. 1996. Oxidative damage to DNA: do
709 we have a reliable biomarker? *Environmental Health Perspectives*. 104, 465–469.
- 710 [49] Hu, K., Yang, M., Xu, Y.Y., Wei, K., Ren, J. 2015. Cell cycle arrest, apoptosis, and
711 autophagy induced by chabamide in human leukemia cells. *Chinese herbal medicine*.8,
712 30-38.

- 713 [50] Debbasch, C., Brignole, F., Pisella, P.J., Warnet, J.M., Rat, P., Baudouin, C. 2001.
714 Quaternary ammoniums and other preservatives' contribution in oxidative stress and
715 apoptosis on Chang conjunctival cells. *Investigative Ophthalmology and Visual*
716 *Science*. 42, 642-652.
- 717 [51] Rjiba-Touati, K., Ayed-Boussema, I., Belarbia, A., Azzebi, A., Achour, A., Bacha, H. 2013.
718 Protective effect of recombinant human erythropoietin against cisplatin cytotoxicity and
719 genotoxicity in cultured Vero cells. *Experimental and Toxicologic Pathology*. 65, 181–
720 187.
- 721 [52] Rello, S., Stockert, J.C., Moreno, V., Gamez, A., Pacheco, M., Juarranz, A., Canete, M.,
722 Villanueva, A. 2005. Morphological criteria to distinguish cell death induced by
723 apoptotic and necrotic treatments. *Apoptosis*. 10, 201-208
- 724 [53] Ndozangue-Touriguine, O., Hamelin, J., Breard, J. 2008. Cytoskeleton and
725 apoptosis. *Biochemical Pharmacology*. 76, 11-18.
- 726 [54] Chaâbane, M., Elwejj, A., Ghorbel, I., Chelly, S., Mnif, H., Boudawara, T., Soudani, N.
727 2018. Penconazole alters redox status, cholinergic function and lung's histoarchitecture
728 of adult rats: Reversal effect of vitamin E. *Biomedicine and Pharmacotherapy*, 102, 645–
729 652.
- 730 [55] Drážovská, M., Šiviková, K., Holečková, B., Dianovský, J., Galdíková, M., and
731 Schwarzbacherová, V. 2016. Evaluation of potential genotoxic/cytotoxic effects induced
732 by epoxiconazole and fenpropimorph-based fungicide in bovine lymphocytes in vitro.
733 *Journal of Environmental Science and Health, Part B*. 51, 769–776.
- 734 [56] Amara, A., Quiniou, F., Durand, G., El Bour, M., Boudabous, A., Hourmant, A.
735 2013. Toxicity of epoxiconazole to the marine diatom *Chaetoceros calcitrans*: influence
736 of growth conditions and algal development stage. *Water, Air & Soil Pollution*. 224, 1–9
- 737 [57] EFSA, (2008). Annual Report on pesticide Residues.
- 738 [58] Deas, E., Cremades, N., Angelova, P.R., Ludtmann, M.H., Yao, Z., Chen, S., Horrocks,
739 M.H., Banushi, B., Little, D., Devine, M.J. 2016. Alpha-synuclein oligomers interact
740 with metal ions to induce oxidative stress and neuronal death in Parkinson's disease.
741 *Antioxidants and Redox Signaling*. 24, 376–391
- 742 [59] Zhao, B. 2009. Natural antioxidants protect neurons in Alzheimer's disease and
743 Parkinson's disease. *Neurochemistry Res*. 34, 630–638.
- 744 [60] Putteeraj, M., Lim, W.L., Teoh, S.L., Yahaya, M.F. 2018. Flavonoids and its
745 neuroprotective effects on brain ischemia and neurodegenerative diseases. *Current Drug*
746 *Targets*. 19, 1710–1720.
- 747 [61] Morais, L., Barbosa-Filho, J., Almeida, R. 2003. Plants and bioactive compounds for the
748 treatment of Parkinson's disease. *Arq. Bras. Fitomedicina Científica*. 1, 127–132.
- 749 [62] Caruana, M., Högen, T., Levin, J., Hillmer, A., Giese, A., Vassallo, N. 2011. Inhibition
750 and disaggregation of α -synuclein oligomers by natural polyphenolic compounds. *FEBS*
751 *Letters*. 585, 1113–1120.
- 752 [63] Stevanovic, T., Diouf, P.N., Garcia-Perez, M.E. 2009. Bioactive polyphenols from
753 healthy diets and forest biomass. *Current Nutrition & Food Science*. 5, 264–295.

754

755

- 756 [64] Parkinson, L., Cicerale, S. 2016. The health benefiting mechanisms of virgin olive oil
757 phenolic compounds. *Molecules*. 21, 1734.
- 758 [65] Angeloni, C., Malaguti, M., Barbalace, M.C., Hrelia, S. 2017. Bioactivity of olive oil
759 phenols in neuroprotection. *International Journal of Molecular Science*. 18, 2230.
- 760 [66] Ong, K.C.; Khoo, H.E. Biological effects of myricetin. *Gen. Pharmacol.* 1997. 29, 121–
761 126.
- 762 [67] Daverey, A and Agrawa, S. K. 2016. Curcumin alleviates oxidative stress and
763 mitochondrial dysfunction in astrocytes. *Neuroscience*. 333, 92-103.
- 764 [68] Scuto, M.C.; Mancuso, C.; Tomasello, B.; Laura Ontario, M.; Cavallaro, A.; Frasca, F.;
765 Maiolino, L.; Trovato Salinaro, A.; Calabrese, E.J.; Calabrese, V. 2019. Curcumin,
766 Hormesis and the Nervous System. *Nutrients*. 11, 2417.
- 767 [69] Calabrese, V.; Santoro, A.; Monti, D.; Crupi, R.; Di Paola, R.; Latteri, S.; Cuzzocrea, S.;
768 Zappia, M.; Giordano, J.; Calabrese, E.J.; et al. 2018. Aging and Parkinson's Disease:
769 Inflammaging, neuroinflammation and biological remodeling as key factors in
770 pathogenesis. *Free Radical Biology and Medicine*. 115, 80–91.
- 771 [70] Brunetti, G., Di Rosa, G., Scuto, M., Leri, M., Stefani, M., Schmitz-Linneweber, C.,
772 Saul, N. 2020. Healthspan Maintenance and Prevention of Parkinson's-like Phenotypes
773 with Hydroxytyrosol and Oleuropein Aglycone in *C. elegans*. *International Journal of*
774 *Molecular Sciences*. 21, 2588.
- 775 [71] Calabrese, V., Cornelius, C., Dinkova-Kostova, A. T., Calabrese, E. J., & Mattson, M. P.
776 2010. Cellular Stress Responses, The Hormesis Paradigm, and Vitagenes: Novel Targets
777 for Therapeutic Intervention in Neurodegenerative Disorders. *Antioxidants & Redox*
778 *Signaling*. 13, 1763–1811.
- 779 [72] Calabrese, E.J.; Calabrese, V.; Giordano, J. 2017. The role of hormesis in the functional
780 performance and protection of neural systems. *Brain Circulation*. 3, 1–13.
- 781 [73] Calabrese, V.; Santoro, A.; Trovato Salinaro, A.; Modafferi, S.; Scuto, M.; Albouchi, F.;
782 Monti, D.; Giordano, J.; Zappia, M.; Franceschi, C.; et al. 2018. Hormetic approaches to
783 the treatment of Parkinson's disease: Perspectives and possibilities. *Journal of*
784 *Neuroscience Resarech*. 96, 1641–1662.
- 785 [74] Di Rosa, G., Brunetti, G., Scuto, M., Trovato Salinaro, A., Calabrese, E. J., Crea, R.,
786 Saul, N. 2020. Healthspan Enhancement by Olive Polyphenols in *C. elegans* Wild Type
787 and Parkinson's Models. *International Journal of Molecular Sciences*, 21, 3893.
- 788 [75] Calabrese, E.J., Calabrese, V., Tsatsakis, A., Giordano, J.J. 2020. Hormesis and Ginkgo
789 biloba (GB): Numerous biological effects of GB are mediated via hormesis. *Ageing*
790 *Research Reviews*
- 791 [76] Williamson MR, Dietrich K, Hackett MJ, et al. 2017. Rehabilitation augments hematoma
792 clearance and attenuates oxidative injury and ion dyshomeostasis after brain
793 hemorrhage. *Stroke*. 48, 195-203.
- 794 [77] Song Y, Bei Y, Xiao Y, Tong HD, Wu XQ, Chen MT. 2018. Edaravone, a free radical
795 scavenger, protects neuronal cells' mitochondria from ischemia by inactivating another
796 new critical factor of the 5-lipoxygenase pathway affecting the arachidonic acid
797 metabolism. *Brain Research*. 1690, 96-104.
- 798 [78] Kang, K.B., Lee, K.H., Chae, S.W., Zhang, R., Jung, M.S., Lee, Y.K., Kim, S.Y., Kim,
799 H.S., Joo, H.G., Park, J.W., Ham, Y.M., Lee, N.H., Hyun, J.W. 2005. Eckol isolated
800 from *Ecklonia cava* attenuates oxidative stress induced cell damage in lung fibroblast
801 cells. *FEBS Letters*. 79, 6295–6304.

- 802 [79] Lei, Y., Chen, J., Zhang, W., Fu, W., Wu, G., Wei, H., Ruan, J. 2012. In vivo
803 investigation on the potential of galangin, kaempferol and myricetin for protection of d-
804 galactose-induced cognitive impairment. *Food Chemistry*. 135, 2702–2707.
- 805 [80] Mansour, S.A., Mossa, A.T.H. 2010. Oxidative damage, biochemical and
806 histopathological alterations in rats exposed to chlorpyrifos and the antioxidant role of
807 zinc. *Pesticide. Biochemistry and Physiology*. 96, 14–23.
- 808 [81] Chen, W., Li, Y., Li, J., Han, Q., Ye, L., Li, A. 2011. Myricetin affords protection against
809 peroxynitrite-mediated DNA damage and hydroxyl radical formation. *Food and
810 chemical toxicology*: 49, 2439–2444.
- 811 [82] Molina-Jimenez, M. F., Sanchez-Reus, M. I., and Benedi, J. 2003. Effect of fraxetin and
812 myricetin on rotenone-induced cytotoxicity in SH-SY5Y cells: Comparison with
813 N-acetylcysteine. *European Journal of Pharmacology*. 472, 81–87.
- 814 [83] Wang, Z. H., Ah Kang, K., Zhang, R., Piao, M. J., Jo, S. H., Kim, J. S., Hyun, J. W.
815 2010. Myricetin suppresses oxidative stress-induced cell damage via both direct and
816 indirect antioxidant action. *Environmental Toxicology and Pharmacology*. 29, 12–18.
- 817 [84] Salvi, M., Battaglia, V., Brunati, A.M., La Rocca, N., Tibaldi, E., Pietrangeli, P.,
818 Marcocci, L., Mondovi, B., Rossi, C.A., Toninello, A. 2007. Catalase takes part in rat
819 liver mitochondria oxidative stress defense. *The Journal of Biological Chemistry*. 282,
820 24407–24415.
- 821 [85] Wu, Y., Chen, H., Li, R., Wang, X., Li, H., Xin, J., Liu, Z., Wu, S., Jiang, W., Zhu, L.
822 2016. Cucurbitacin-I induces hypertrophy in H9c2 cardiomyoblasts through activation of
823 autophagy via MEK/ERK1/2 signaling pathway. *Toxicology Letters*. 264, 87–98.
- 824 [86] Calabrese, V., Renis, M., Calderone, A., Russo, A., Barcellona, M. L., & Rizza, V.
825 1996. Stress proteins and SH-groups in oxidant-induced cell damage after acute ethanol
826 administration in rat. *Free Radical Biology and Medicine*. 20, 391–397.
- 827 [87] Calabrese, V., Cornelius, C., Maiolino, L., Luca, M., Chiaramonte, R., Toscano, M. A.,
828 & Serra, A. 2010. Oxidative Stress, Redox Homeostasis and Cellular Stress Response in
829 Ménière's Disease: Role of Vitagenes. *Neurochemical Research*. 35, 2208–2217.
- 830 [88] Calabrese, E., Iavicoli, I., & Calabrese, V. 2012. Hormesis. *Human & Experimental
831 Toxicology*. 32, 120–152.
- 832 [89] Calabrese, V.; Santoro, A.; Trovato Salinaro, A.; Modafferi, S.; Scuto, M.; Albouchi, F.;
833 Monti, D.; Giordano, J.; Zappia, M.; Franceschi, C.; et al. 2018. Hormetic approaches to
834 the treatment of Parkinson's disease: Perspectives and possibilities. *Journal of
835 Neuroscience Research*. 96, 1641–1662.
- 836 [90] Peters, V., Calabrese, V., Forsberg, E., Volk, N., Fleming, T., Baelde, H., Schmitt, C.
837 2018. Protective Actions of Anserine Under Diabetic Conditions. *International Journal
838 of Molecular Sciences*. 19, 2751.
- 839 [91] Pilipenko, V., Narbutė, K., Amara, I., Trovato, A., Scuto, M., Pupure, J., Calabrese, V.
840 2019. GABA-containing compound gammapyrone protects against brain impairments in
841 Alzheimer's disease model male rats and prevents mitochondrial dysfunction in cell
842 culture. *Journal of Neuroscience Research*. 97, 708–726.
- 843 [92] Leri, M., Scuto, M., Laura Ontario, M., Calabrese, V., Calabrese, E.J., Bucciantini, M.,
844 and Stefani, M. 2020. Healthy Effects of Plant Polyphenols: Molecular Mechanisms.
845 *International Journal of Molecular Sciences*. 21, 1250
- 846 [93] Federico, A., Cardaioli, E., Da Pozzo, P., Formichi, P., Gallus, G.N., Radi, E.
847 2012. Mitochondria, oxidative stress and neurodegeneration. *Journal of Neurological
848 Science*. 322, 254–262.

- 849 [94] D'Autréaux, B., Toledano, MB. 2007. ROS as signaling molecules: mechanisms that
850 generate specificity in ROS homeostasis. *NatureReviewMolecular Cellular Biology*.8,
851 813-824.
- 852 [95] Rigoulet, M.,Yoboue, ED., Devin, A. 2011.Mitochondrial ROS generation and its
853 regulation: mechanisms involved in H₂O₂ signaling. *Antioxidant Redox Signal*.14, 459-
854 468.
- 855 [96] Wu, S., Yue, Y., Peng, A., Zhang, L., Xiang, J., Cao, X., Ding, H., Yin, S. 2016.
856 Myricetin ameliorates brain injury and neurological deficits 2 via Nrf2 activation after
857 experimental stroke in middle-aged rats. *Food and Function*. 1-28.
- 858 [97] Zou, D., Liu, P., Chen, K., Xie, Q., Liang, X., Bai, Q., et al. 2015. Protective Effects of
859 Myricetin on Acute Hypoxia-Induced Exercise Intolerance and Mitochondrial
860 Impairments in Rats.*PLoS ONE*.104, e0124727.
- 861 [98] Choi, C.S., Savage, D.B., Kulkarni, A., Yu, X.X., Liu, Z.X., Morino, K., et al.
862 2007.Suppression of diacylglycerol acyltransferase-2 (DGAT2), but not DGAT1, with
863 antisense oligonucleotides reverses diet-induced hepatic steatosis and insulin resistance.
864 *Journal of Biological Chemistry*.282, 22678–88.
- 865 [99] Copple, I.M., Goldring, C.E., Kitteringham, N.R., Park, B.K. 2008. The Nrf2-Keap1
866 defence pathway: role in protection against drug-induced toxicity. *Toxicology*. 246, 24–
867 33.
- 868 [100] Satoh, T., Okamoto, S.I., Cui, J., Watanabe, Y., Furuta, K., Suzuki, M., et al.
869 2006.Activation of the Keap1/Nrf2 pathway for neuroprotection by electrophilic
870 [correction of electrophillic] phase II inducers.*Proceedings of the National Academy of
871 Sciences Proceedings of the National Academy of Sciences of the United States of
872 America*.103, 768–73.
- 873 [101] Simmons, E.; Scholpa, N.; Schnellmann, R. 2020.Mitochondrial biogenesis as a
874 therapeutic target for traumatic and neurodegenerative CNS diseases. *Experimental
875 Neurology*. 329, 113-309.
- 876 [101] Ventura-Clapier, R., Garnier, A.,Veksler, V. 2008. Transcriptional control of
877 mitochondrial biogenesis: the central role of PGC-1alpha. *Cardiovascular
878 Research*. 79, 208-217
- 879 [102] Jornayvaz, F.R., Shulman, G.I. 2010. Regulation of mitochondrial biogenesis. *Essays
880 in Biochemistry* . 47, 69-84
- 881 [103] Hock, M.B., Kralli, A. 2009. Transcriptional control of mitochondrial biogenesis and
882 function.*Annual Review of Physiology*. 71, 177-203.
- 883 [104] Virbasius, J.V., Scarpulla, R.C.1994. Activation of the human mitochondrial
884 transcription factor A gene by nuclear respiratory factors: a potential regulatory link
885 between nuclear and mitochondrial gene expression in organelle biogenesis. *Proceedings
886 of the National Academy of Sciences Proceedings of the National Academy of Sciences
887 of the United States of America*. 91, 1309-1313.
- 888 [105] Kelly, D. P., & Scarpulla, R. C. 2012. Transcriptional Control of Striated Muscle
889 Mitochondrial Biogenesis and Function. *Muscle*, 203–215.
- 890 [106] Krepela, E. 2001.Cysteine proteinases in tumor cell growth and apoptosis.*Neoplasma*.
891 48, 332–349.
- 892 [107] Van Acker, S.A., de Groot, M.J., van den Berg, D.J., Tromp, M.N., DonneOp den
893 Kelder, G., van der Vijgh, W.J., Bast, A. 1996. A quantum chemical explanation of the
894 antioxidant activity of flavonoids.*Chemical Research in Toxicology*. 9, 1305 – 1312.

- 895 [108] Paya, M., Ferrandiz, M.L., Miralles, F., Montesinos, C., Ubeda, A., Alcaraz, M.J.,
896 1993. Effects of coumarin derivatives on superoxide anion
897 generation. *Arzneimittelforschung* 43, 655 – 658.
- 898 [109] Chobot, V., Hadacek, F. 2011. Exploration of pro-oxidant and antioxidant activities of
899 the flavonoid myricetin. *Redox Report*. 16, 242-247.
- 900

901 **6. Figure legends**

902 **Fig.1. Cytotoxic effect of Epoxiconazole on F98 cells and the protective effect of the two**
903 **hours Myricetin pre-treatment.**

904 (A) Cells were treated with EPX and MYR separately at the indicated concentrations during
905 24 h. Cell viability was determined using the MTT assay and expressed as percentages of
906 viability. Values are significantly different ($p < 0.05$) from control ($n = 5$).

907 (B) Cells were pretreated for 2 h with MYR before adding EPX (50 μ M). Cell morphology
908 was visualized microscopically and then photographed using IncuCyte® Live-Cell Analysis.

909 (C) Cells were treated with EPX (50 μ M) and MYR (10, 20, 50 μ M). Data are expressed as
910 the mean \pm SD of three separate experiments. $^{##}P < 0.01$ vs. control $^{**}P < 0.01$ and $^{*}P < 0.05$
911 vs. EPX alone.

912 (D) Effects of MYR on EPX-induced cell cycle arrest. F98 cells were pre-treated during 2
913 hours with MYR (10, 20 and 50 μ M) before the EPX treatment for 24 h (50 μ M). The cell
914 cycle arrest was analyzed by flow cytometric analysis. Percentages of cells in different phases
915 of the Cell Cycle were measured and expressed as the Mean \pm SD of three separate
916 experiments. $^{##}P < 0.01$ and $^{###}P < 0.001$ vs. control, $^{**}P < 0.01$ and $^{*}P < 0.05$ vs. EPX alone.
917 The triangle indicates the increasing concentrations of MYR (10, 20 and 50 μ M).

918 **Fig.2. Protective effects of Myricetin on the Epoxiconazole-induced oxidative stress.**

919 (A) Cells were pre-treated with MYR (10, 20 and 50 μ M) for 2 h before EPX treatment for 24
920 h (50 μ M). The relative intracellular ROS production was evaluated by recording the
921 fluorescence of DCF, the product of DCFH oxidation mainly by H_2O_2 . H_2O_2 , at 20 μ M and
922 NAC at 1mM, were used as positive controls. Data are expressed as the mean \pm SD of three
923 separate experiments. $^{##}P < 0.01$, $^{###}P < 0.001$ vs. control, $^{**}P < 0.01$ and $^{***}P < 0.001$ vs.
924 EPX alone.

925 (B) Effects of MYR on EPX-induced lipid peroxidation. Cells were pre-treated with MYR
926 (10, 20 and 50 μ M) for 2 h before EPX treatment for 24h (50 μ M). The peroxidation of lipids
927 was recorded by measuring the accumulation of MDA. H_2O_2 , at 20 μ M and NAC at 1mM,
928 were used as positive controls. Data are expressed as the mean \pm SD of three separate
929 experiments. $^{###}P < 0.001$ vs. control, $^{*}P < 0.05$, $^{**}P < 0.01$ and $^{***}P < 0.001$ vs. EPX alone.

930 (C and D) Effects of MYR on catalase and superoxide dismutase activities. Cells were pre-
931 treated with MYR (10, 20 and 50 μ M) for 2 h before EPX treatment for 24 h (50 μ M). H_2O_2 ,
932 at 20 μ M and NAC at 1mM, were used as positive controls. Data are expressed as the mean \pm
933 SD of three separate experiments. $^{###}P < 0.001$ vs. control, $^{**}P < 0.01$, $^{*}P < 0.05$ and $^{***}P <$
934 0.001 vs. EPX alone.

935 **Fig.3. Effects of Myricetin on the Epoxiconazole-induced DNA damage, caspases**
936 **activation, mitochondrial trans-membrane potential ($\Delta\Psi_m$) and externalization of**
937 **Phosphatidylserine.**

938 (A) Cells were pre-treated with MYR (10, 20 and 50 μ M) for 2 h before EPX treatment for 24
939 h (50 μ M). Data are expressed as the mean \pm SD of three separate experiments. ^{##}P < 0.01 vs.
940 control, ^{**}P < 0.01 vs. EPX alone.

941 (B) Effects of MYR on EPX-induced caspase-3 activation. Data are expressed as the mean \pm
942 SD of three separate experiments. ^{###}P < 0.001 vs. control, ^{*}P < 0.05 and ^{**}P < 0.01 vs. EPX
943 alone.

944 (C) The effect of Z-VAD-FMK pretreatment (2 h, 50 μ M) on EPX-induced cytotoxicity. Data
945 are expressed as the mean \pm SD of three independent experiments. (^αP < 0.05) values are
946 significantly different from Z-vad-fmk pretreated cells.

947 (D) Effects of MYR on EPX-induced caspase-9 activation. Data are expressed as the Mean \pm
948 SD of three separate experiments. ^{###}P < 0.001 vs. control, ^{*}P < 0.05 and ^{***}P < 0.001 vs. EPX
949 alone.

950 (E) Different subsets of cells were measured by AnnexinV/PI staining after treatment with
951 EPX (50 μ M) and/or MYR (10, 20 and 50 μ M). The rate of apoptosis is the sum of the early
952 and late apoptosis. Data are expressed as the mean \pm SD of three separate experiments. ^{###}P
953 < 0.001 vs. control, ^{*}P < 0.05, ^{**}P < 0.01 and ^{***}P < 0.001 vs. EPX alone. (^βP < 0.01) values
954 are significantly different from Z-LEHD-FMK pretreated cells.

955 (F) Effects of MYR on EPX-induced loss of mitochondrial trans-membrane potential ($\Delta\Psi_m$).
956 F98 cells were pre-treated with MYR (10, 20 and 50 μ M) for 2 h before EPX treatment for 24
957 h (50 μ M). The mitochondrial potential was assessed by measuring the uptake of Rhodamine-
958 123. Data are expressed as the mean \pm SD of three separate experiments. ^{##}P < 0.01 vs.
959 control, ^{*}P < 0.05 vs. EPX alone.

960 **Fig.4. Effects of Epoxiconazole and Myricetin on the cytoskeleton, chromatin and**
961 **mitochondria of rat F98 cells.**

962 Microtubules (A) and intermediate filaments (B) were detected using respectively an anti-
963 Tubulin and an anti-Vimentin antibody. Cells were examined with a confocal microscope.
964 Cells treated with 50 μ M EPX lack a normal cytoskeleton network and typically adopt a
965 spherical shape, while the pre-treatment with MYR strongly reduced this effect.

966 **Fig.5. Graphical abstract**

967 A proposed mechanism of pretreatment with Myricetin in alleviating Epoxiconazole-induced
968 neurotoxicity. The protective effect is mainly attributed to its ability to reduce intracellular

969 reactive oxygen levels, modulating the antioxidant enzymes activity, reducing
970 malondialdehyde level, stabilizing the cytoskeleton organization and mitochondrial membrane
971 potential. Finally, Myricetin pretreatment prevented the increase of DNA
972 fragmentation, caspases-3 and 9 activities and DNA condensation.

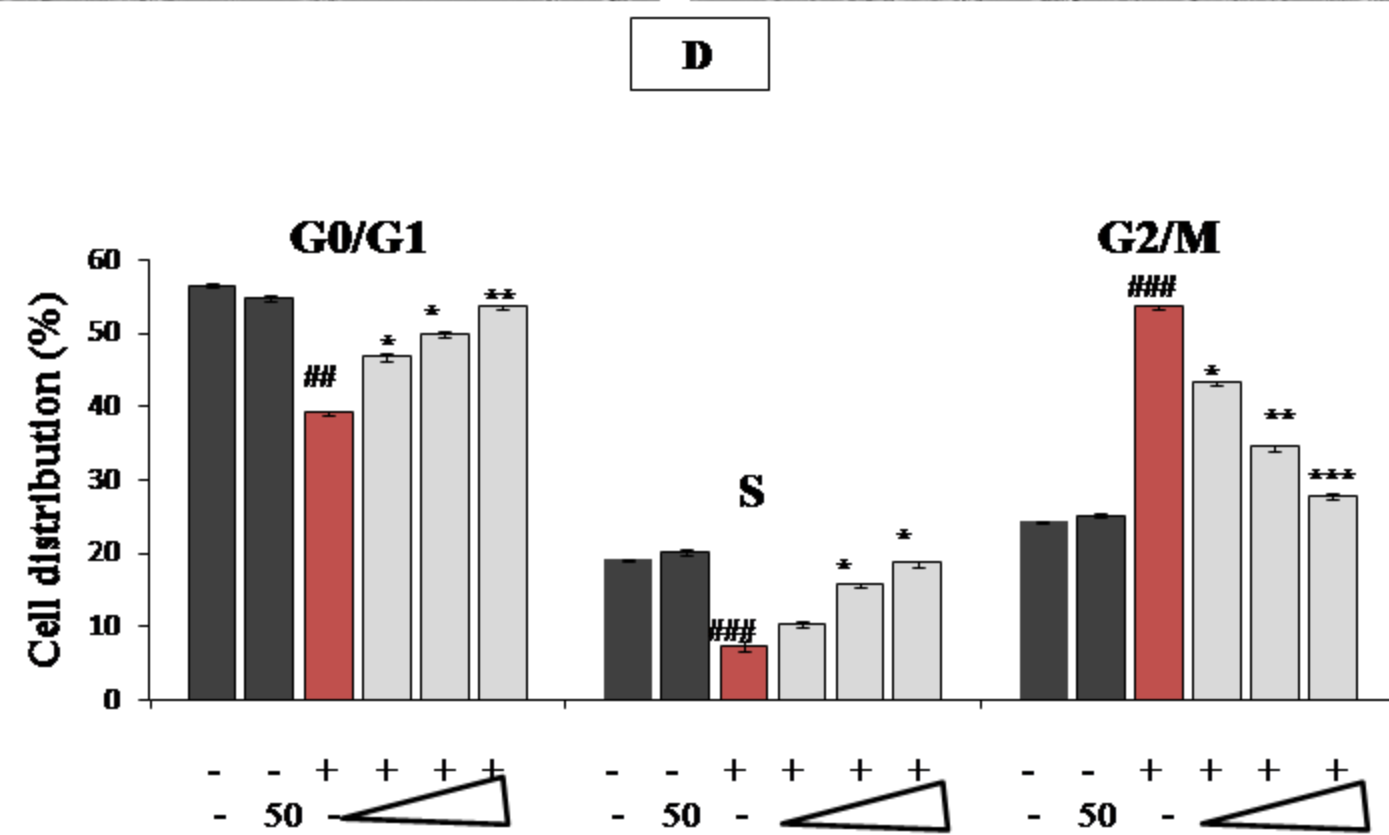
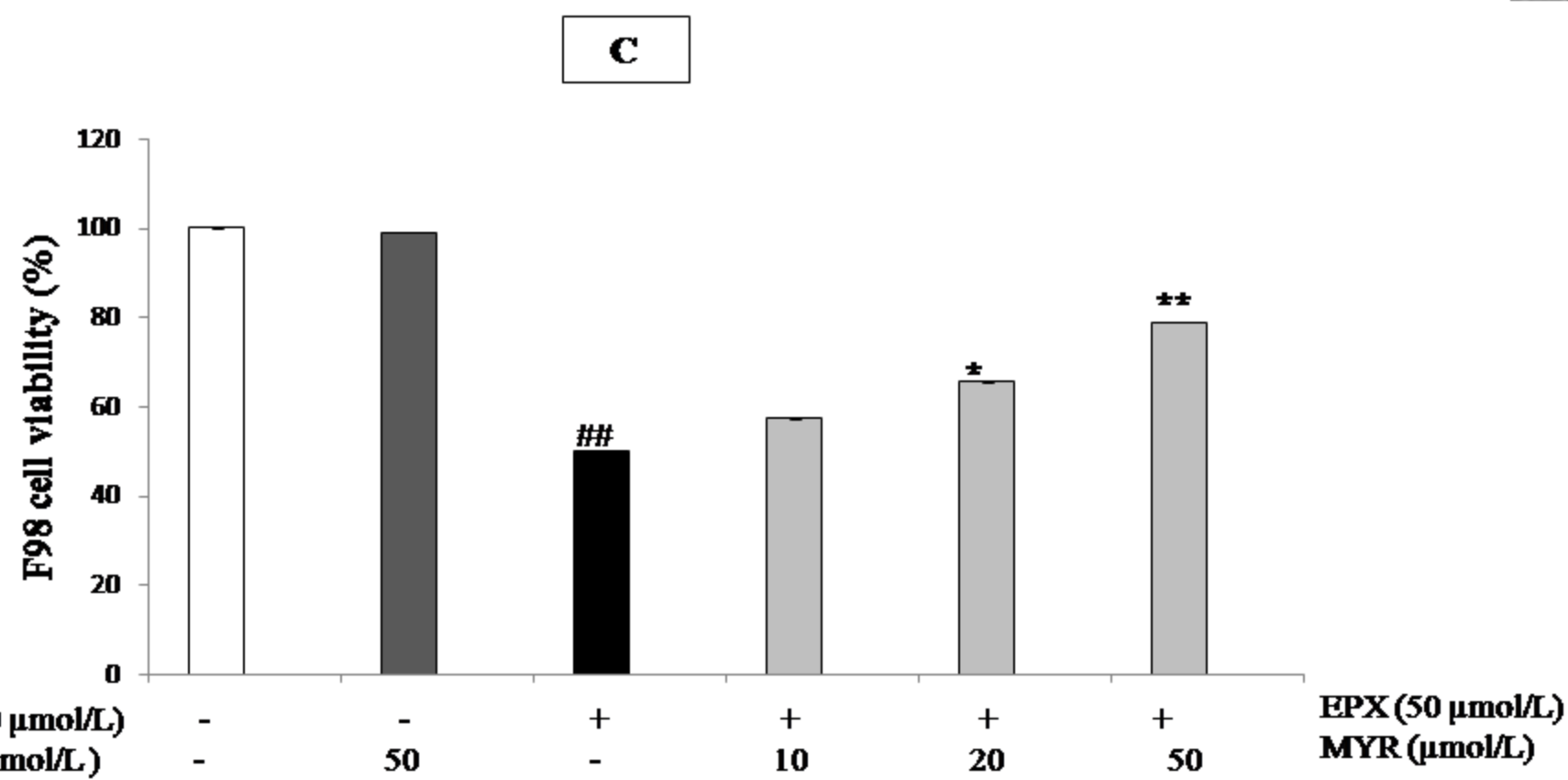
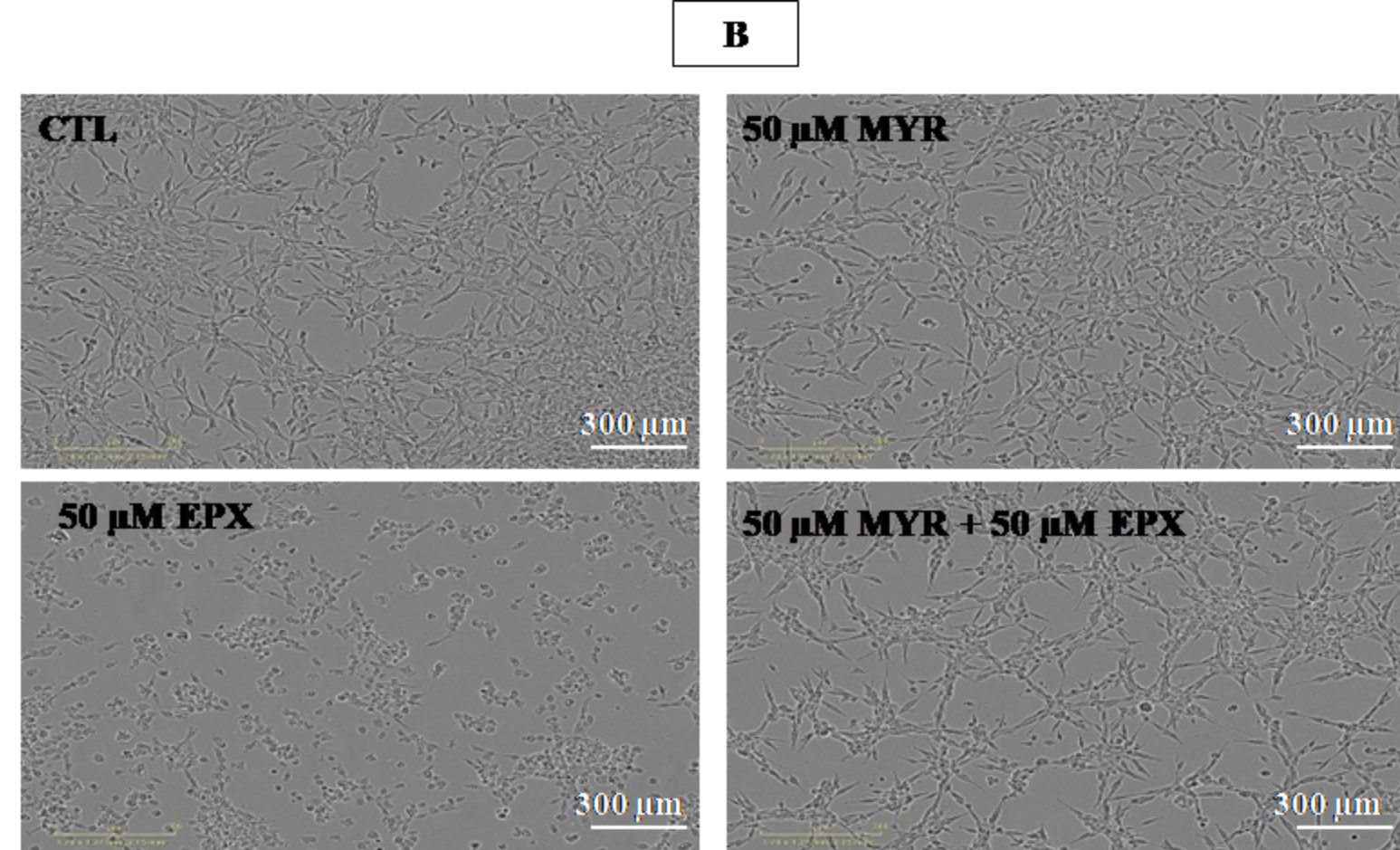
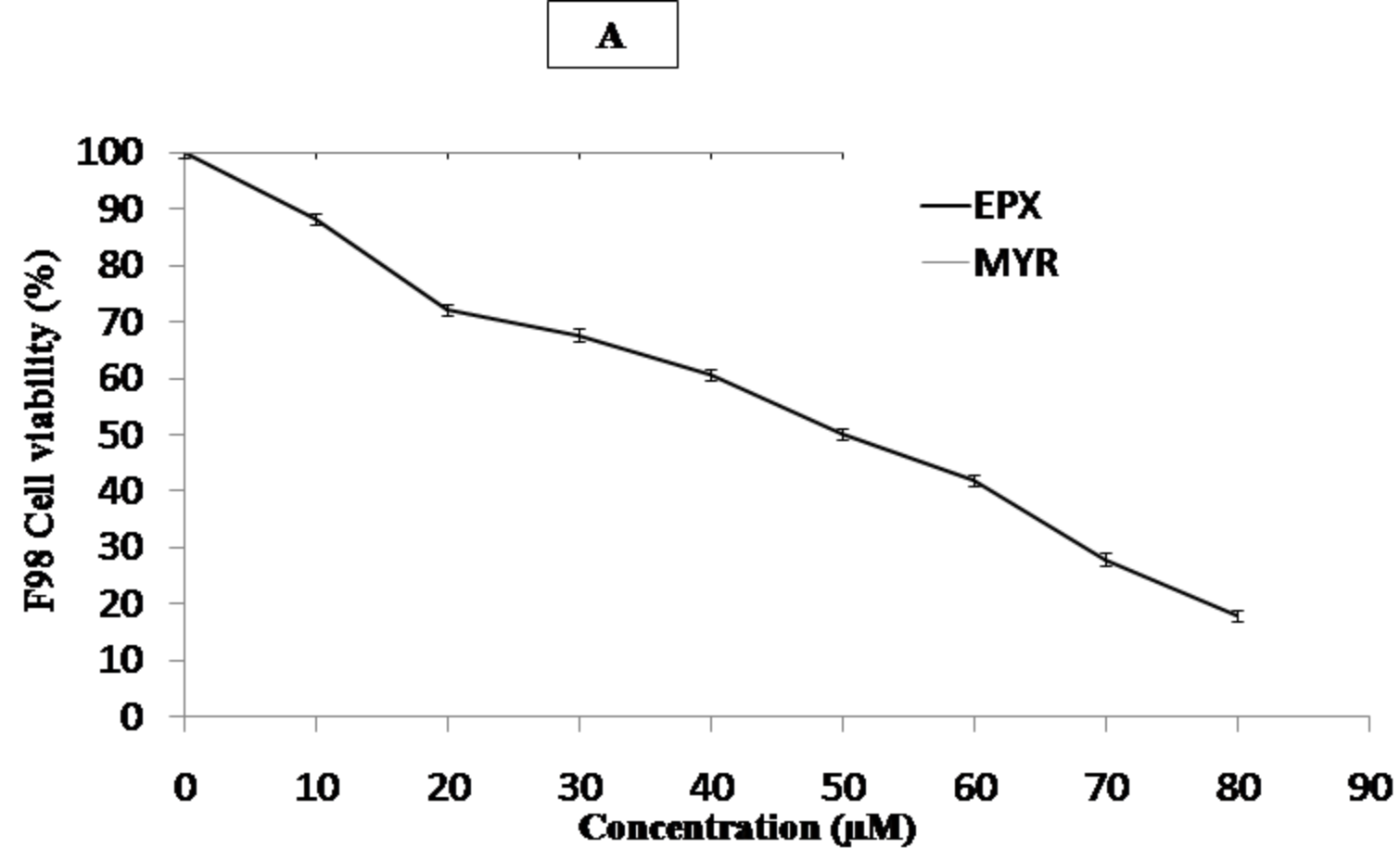


Fig. 1

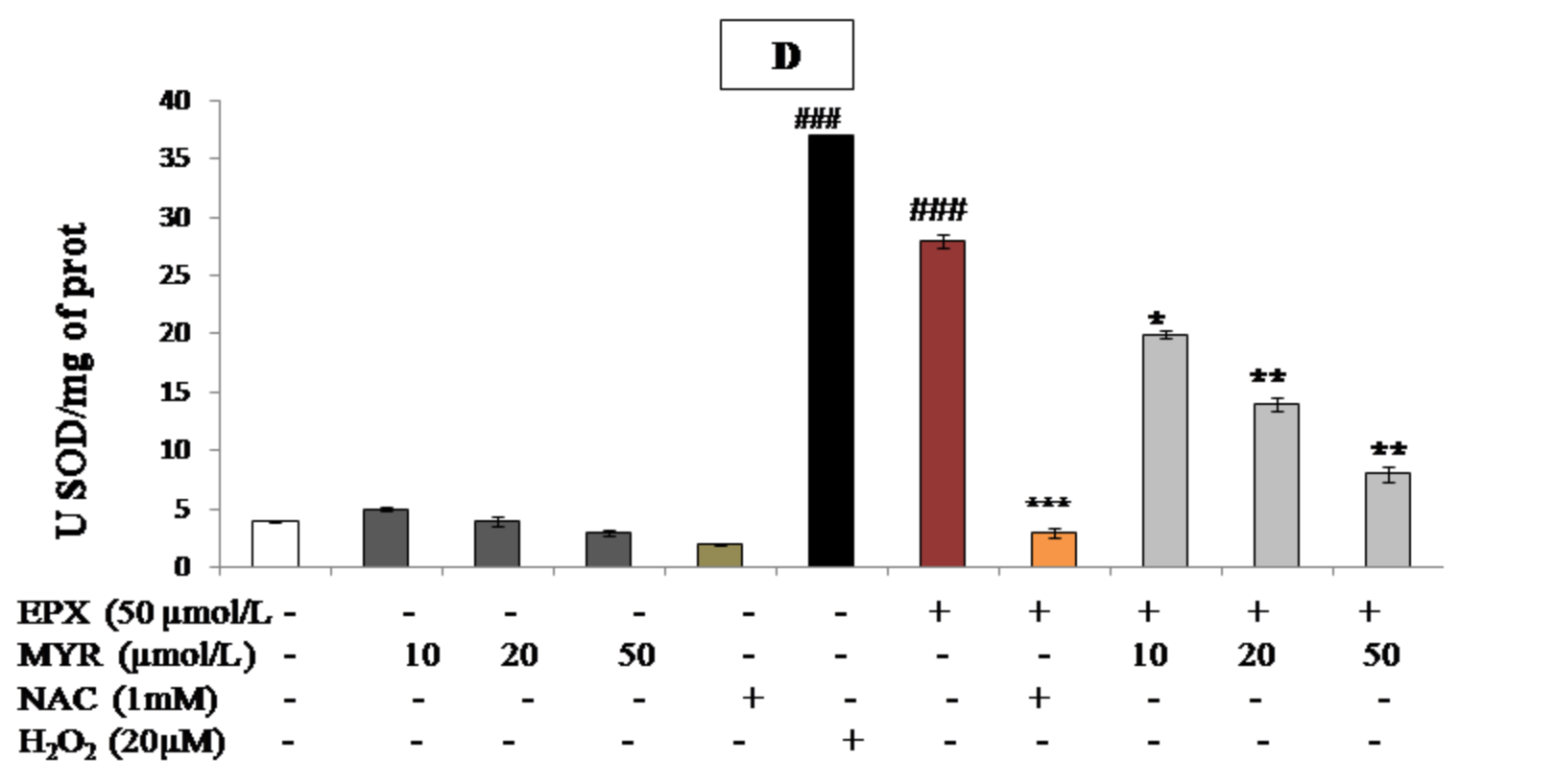
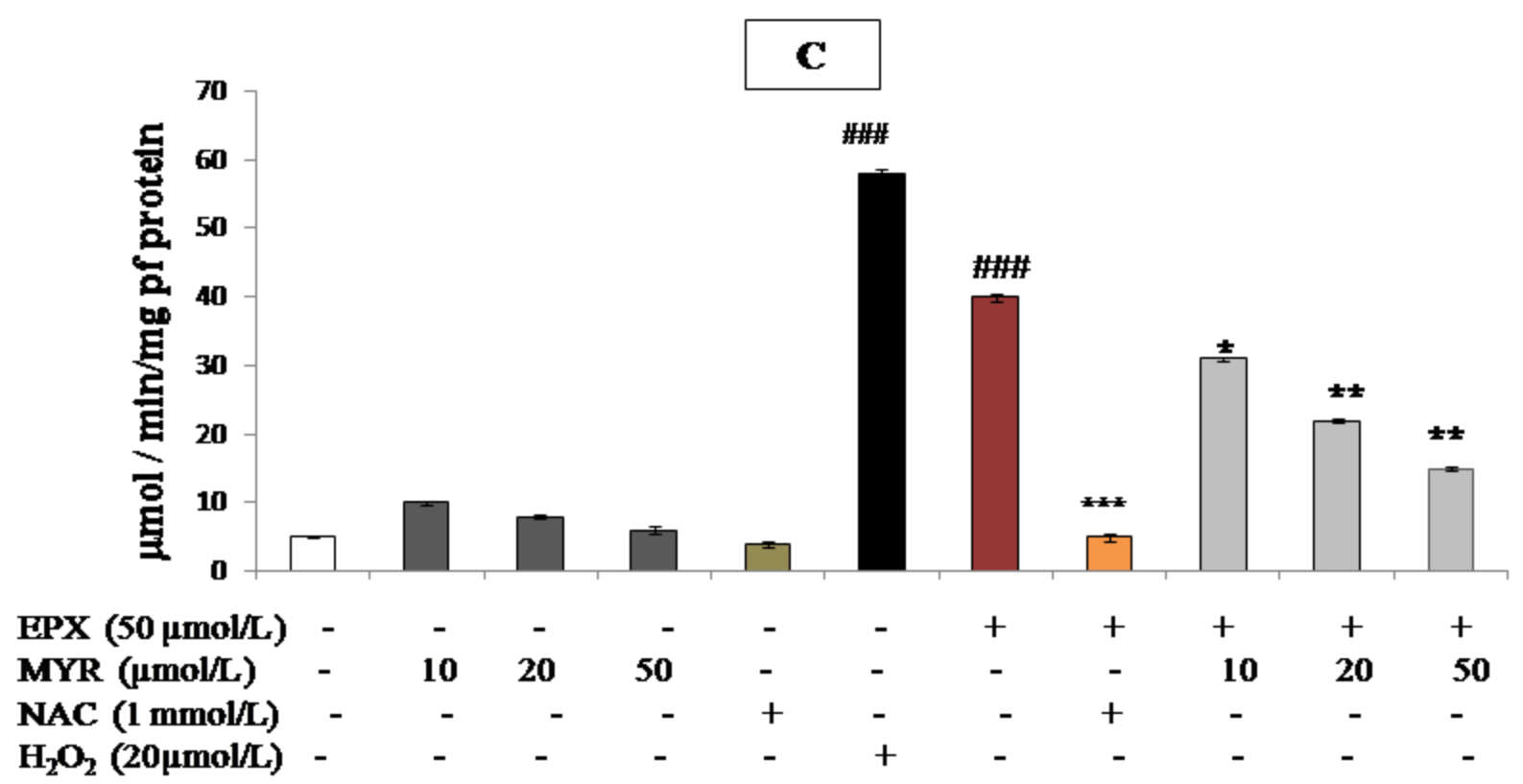
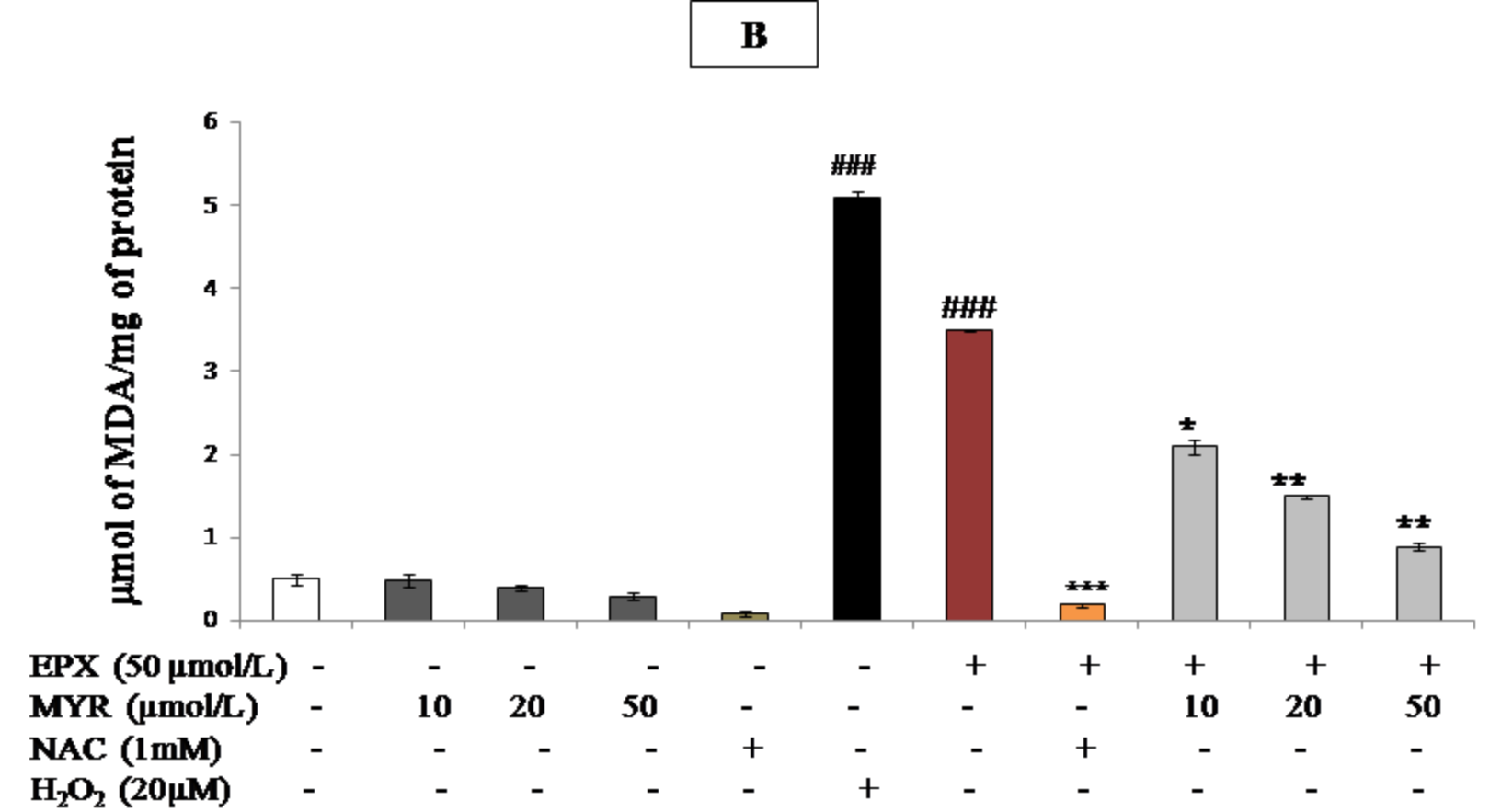
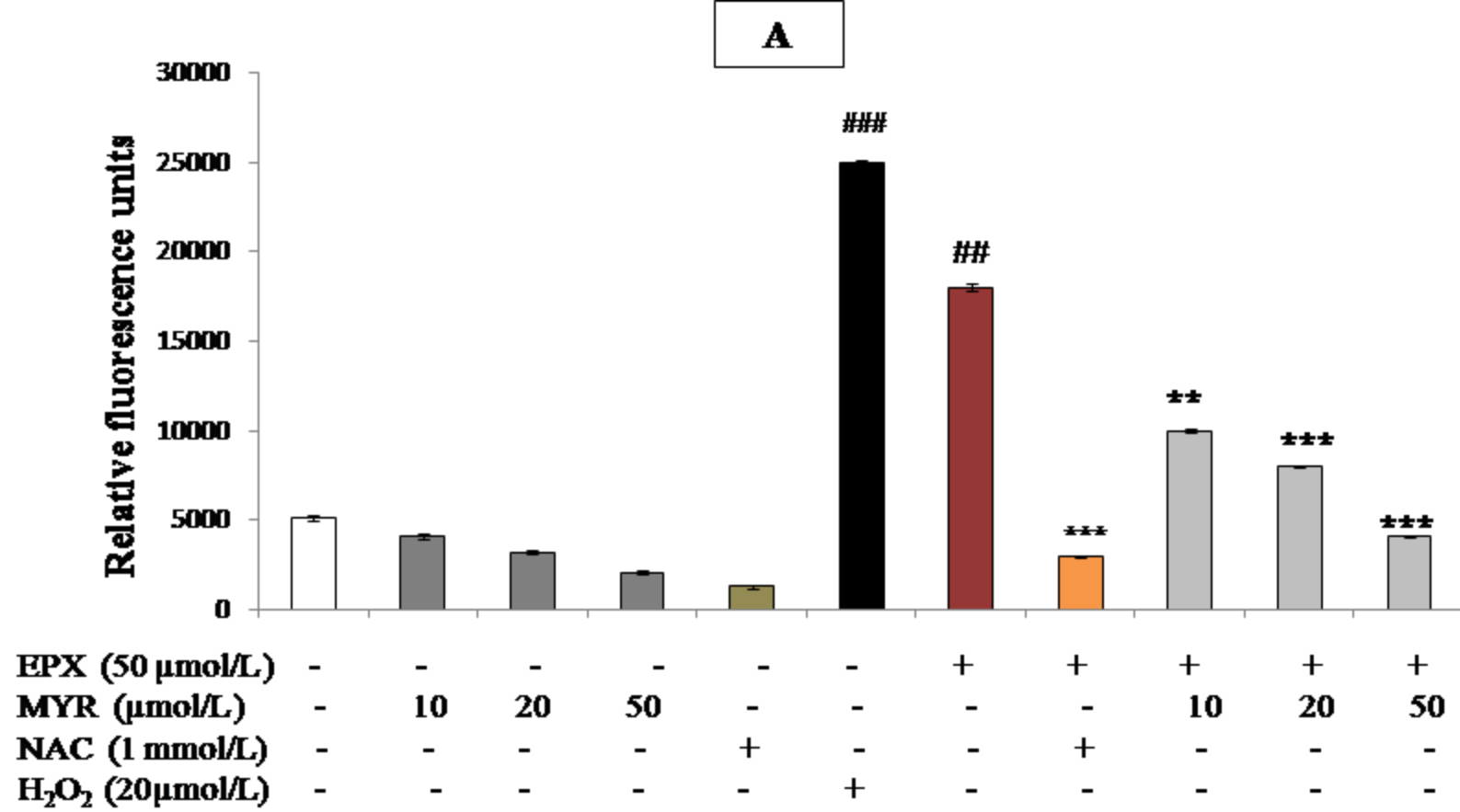


Fig. 2

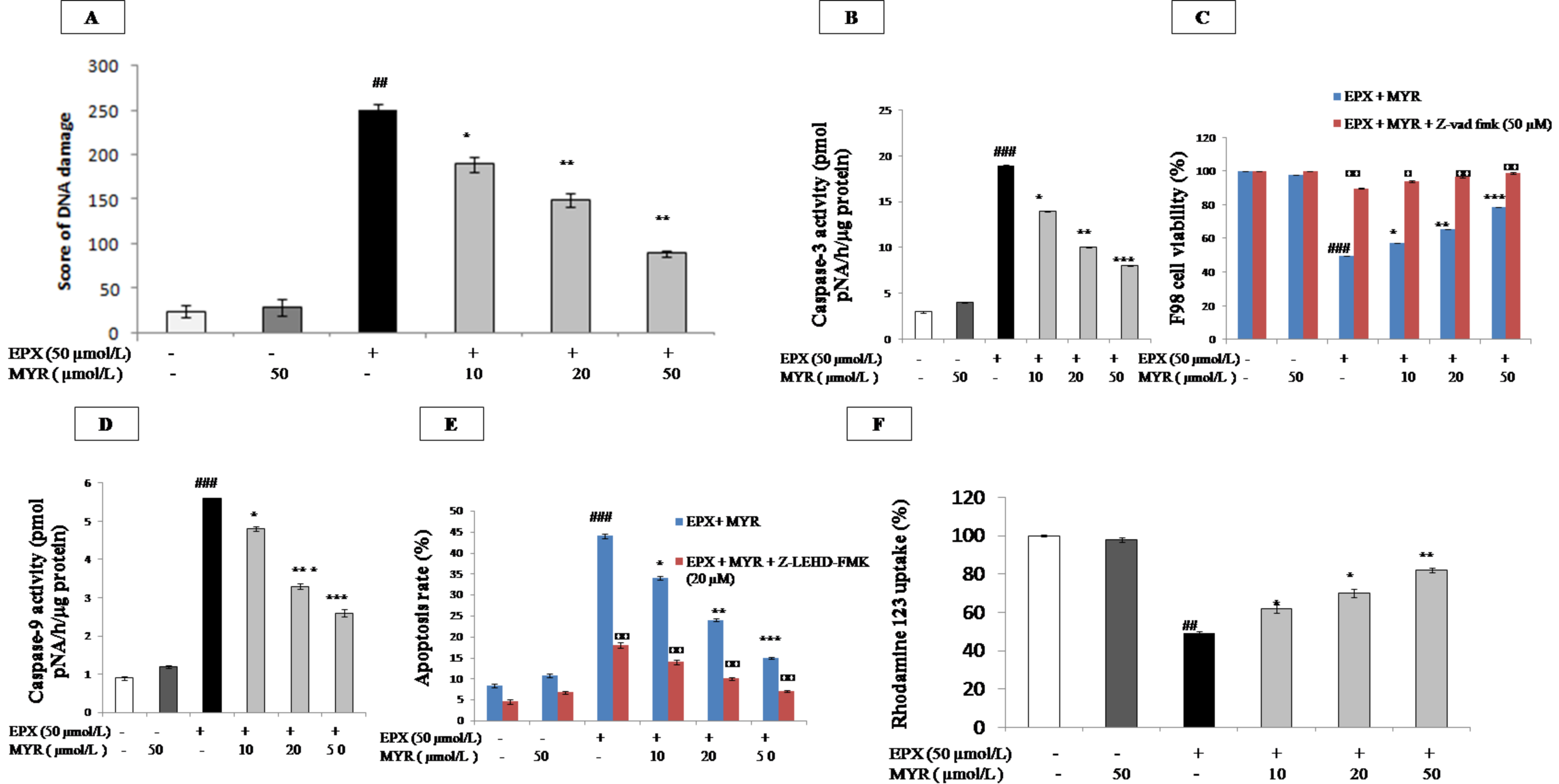
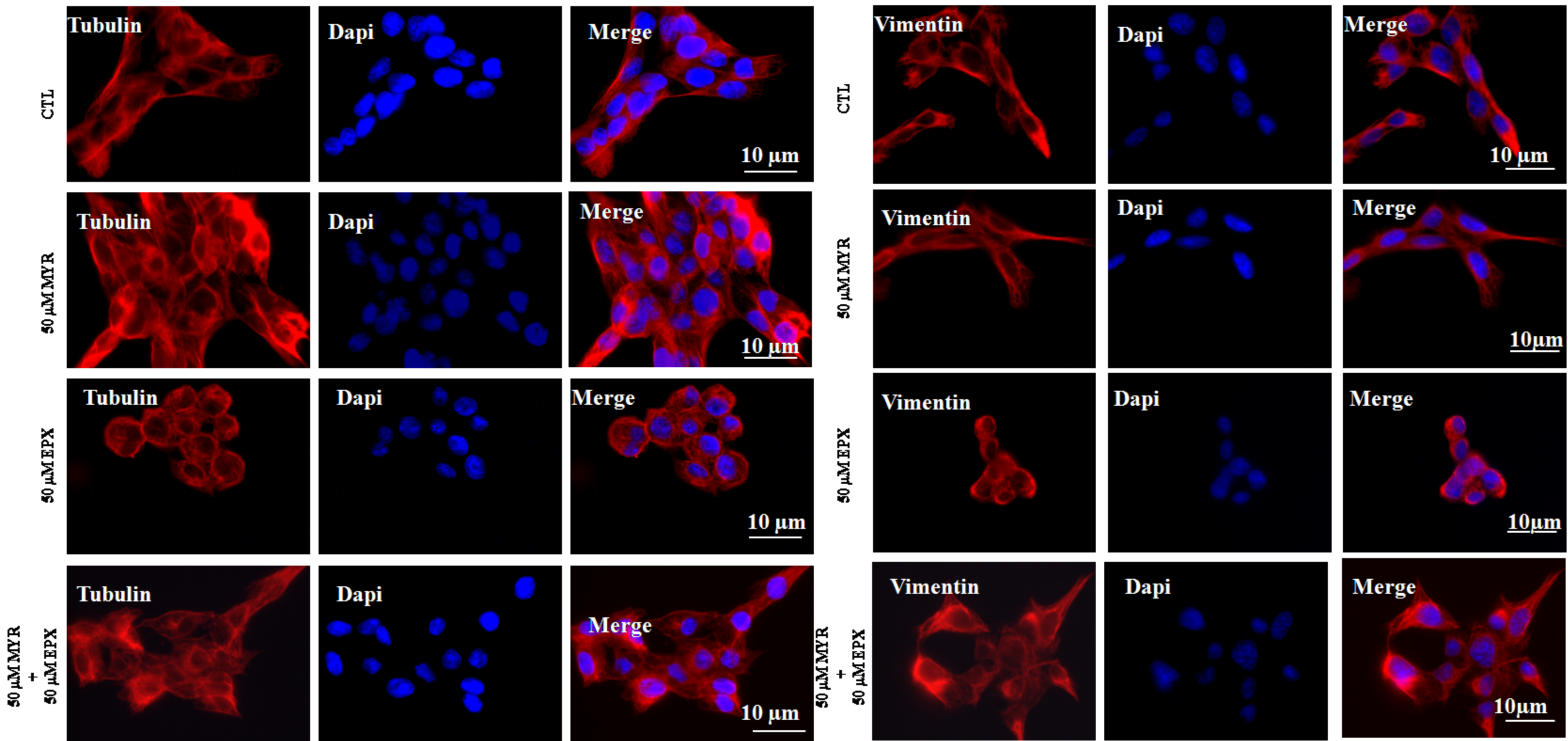


Fig. 3

A**B****Fig. 4**

